SAND99-1882J

Characterization of Stochastic Uncertainty in the 1996 Performance Assessment for the Waste Isolation Pilot Plant

J.C. Helton[a], F.J. Davis[b], J.D. Johnson[c]

[a]Department of Mathematics, Arizona State University, Tempe, AZ 85287 USA

[b]Sandia National Laboratories, Albuquerque, NM 87185 USA

[c]GRAM, Inc., Albuquerque, NM 87112 USA

Abstract

The 1996 performance assessment (PA) for the Waste Isolation Pilot Plant (WIPP) maintains a separation between stochastic (i.e., aleatory) and subjective (i.e., epistemic) uncertainty, with stochastic uncertainty arising from the possible disruptions that could occur at the WIPP over the 10,000 yr regulatory period specified by the U.S. Environmental Protection Agency (40 CFR 191, 40 CFR 194) and subjective uncertainty arising from an inability to uniquely characterize many of the inputs required in the 1996 WIPP PA. The characterization of stochastic uncertainty is discussed, including drilling intrusion time, drilling location, penetration of excavated/nonexcavated areas of the repository, penetration of pressurized brine beneath the repository, borehole plugging patterns, activity level of waste, and occurrence of potash mining. Additional topics discussed include sampling procedures, generation of individual 10,000 yr futures for the WIPP, construction of complementary cumulative distribution functions (CCDFs), mechanistic calculations carried out to support CCDF construction, the Kaplan/Garrick ordered triple representation for risk, and determination of scenarios and scenario probabilities.

Key Words: Aleatory uncertainty, complementary cumulative distribution function, compliance certification application, epistemic uncertainty, Latin hypercube sampling, performance assessment, radioactive waste, random sampling, scenario, stochastic uncertainty, subjective uncertainty, transuranic waste, Waste Isolation Pilot Plant, 40 CFR 191, 40 CFR 194.

Please send page proof to:

Jon C. Helton
Department 6848, MS 0779
Sandia National Laboratories
Albuquerque, NM 87185-0779, USA
Phone: 505-284-4808
Fax: 505-844-2348
email: jchelto@sandia.gov

DISCLAIMER

1. Introduction

At a conceptual level, the 1996 performance assessment (PA) for the Waste Isolation Pilot Plant (WIPP) is underlain by three entities (EN1, EN2, EN3): EN1, a probabilistic characterization of the likelihood of different futures occurring at the WIPP site over the next 10,000 yr (Sect. 3, Ref. 1); EN2, a procedure for estimating the radionuclide releases to the accessible environment associated with each of the possible futures that could occur at the WIPP site over the next 10,000 yr (Sect. 4, Ref. 1); and EN3, a probabilistic characterization of the uncertainty in the parameters used in the definition of EN1 and EN2 (Sect. 5, Ref. 1). The first entity, EN1, and its role in the 1996 WIPP PA is the primary focus of this article.

When viewed formally, EN1 is defined by a probability space $(S_{st}, \mathcal{S}_{st}, p_{st})$ for stochastic uncertainty (Sect. 3, Ref. 1). Further, the elements $\mathbf{x}_{st}$ of the sample space S_{st} are vectors of the form

$$\mathbf{x}_{st} = [\underbrace{t_1, l_1, e_1, b_1, p_1, \mathbf{a}_1}_{1^{st}\text{ intrusion}}, \underbrace{t_2, l_2, e_2, b_2, p_2, \mathbf{a}_2}_{2^{nd}\text{ intrusion}}, \ldots, \underbrace{t_n, l_n, e_n, b_n, p_n, \mathbf{a}_n}_{n^{th}\text{ intrusion}}, t_{min}], \tag{1}$$

where n is the number of drilling intrusions in the vicinity of the repository, t_i is the time (yr) of the i^{th} intrusion, l_i designates the location of the i^{th} intrusion, e_i designates the penetration of an excavated or nonexcavated area by the i^{th} intrusion, b_i designates where or not the i^{th} intrusion penetrates pressurized brine in the Castile Formation, p_i designates the plugging procedure used with the i^{th} intrusion (i.e., continuous plug, two discrete plugs, three discrete plugs), $\mathbf{a}_i$ designates the type of waste penetrated by the i^{th} intrusion (i.e., no waste, contact-handled (CH) waste, remotely-handled (RH) waste), and t_{min} is the time at which potash mining occurs within the land withdrawal boundary (Sect. 3, Ref. 1). The manner in which the individual components t_i, l_i, e_i, b_i, p_i, $\mathbf{a}_i$ and t_{min} of $\mathbf{x}_{st}$ are defined in the 1996 WIPP PA is described (Sects. 2 - 8). The definitions of these components and their associated probability distributions give rise to the probability space $(S_{st}, \mathcal{S}_{st}, p_{st})$ for stochastic uncertainty. The preliminary work that lead to these definitions was carried out as part of an extensive review of features, events and processes (FEPs) that could occur at the WIPP.[2]

Sampling from the probability spaces $(S_{st}, \mathcal{S}_{st}, p_{st})$ and $(S_{su}, \mathcal{S}_{su}, p_{su})$ for stochastic (i.e., aleatory) and subjective (i.e., epistemic) uncertainty plays an important role in the 1996 WIPP PA (Sects. 3, 4, Ref. 1). In particular, the complementary cumulative distribution function (CCDF) used in comparisons with the boundary line specified in 40 CFR 191.13(a) (Refs. 3, 4) is defined and then approximated by

$$prob(Rel > R) = \int_{S_{st}} \delta_R\left[f(\mathbf{x}_{st})\right] d_{st}(\mathbf{x}_{st})\, dV_{st} \doteq \sum_{i=1}^{nS} \delta_R\left[f(\mathbf{x}_{st,i})\right] / nS, \tag{2}$$

where $\mathbf{x}_{st,i}$, $i = 1, 2, \ldots, nS$, is a random sample of size nS from S_{st} generated in consistency with the probabilistic relationships that define $(S_{st}, \mathcal{S}_{st}, p_{st})$, f is the function that gives the normalized release to the accessible environment associated with each sample element $\mathbf{x}_{st,i}$, and $\delta_R[f(\mathbf{x}_{st,i})] = 1$ if $f(\mathbf{x}_{st,i}) > R$ and 0 if $f(\mathbf{x}_{st,i}) \leq R$ (Sect. 3, Ref. 1). Therefore, sampling procedures are discussed (Sect. 9). Then, the generation of samples from $(S_{st}, \mathcal{S}_{st}, p_{st})$ and their use in the construction of CCDFs for comparison with the boundary line specified in 40 CFR 191.13(a) are described (Sects. 11 - 13).

To provide perspective on the treatment of stochastic uncertainty in the 1996 WIPP PA and other analyses, descriptions are provided for the Kaplan and Garrick ordered triple representation for risk[5] and its relationship to the treatment of stochastic uncertainty in the 1996 WIPP PA (Sect. 13). Further, the definition of scenarios and scenario probabilities in the context of the probability space $(S_{st}, \mathcal{S}_{st}, p_{st})$ are also described (Sect. 14). Finally, a concluding discussion is given (Sect. 15).

This article is based on material contained in Chapts. 3 and 6 of Ref. 6.

2. Drilling Intrusion Time t_i

Drilling intrusions in the 1996 WIPP PA are assumed to occur randomly in time and space (i.e., follow a Poisson process; Refs. 7 - 9). Specifically, the base drilling rate considered within the area marked by a berm as part of the system for passive institutional controls (Fig. 1) is 46.8 intrusions/km^2/10^4 yr (App. DEL, Ref. 10). Further, active institutional controls are assumed to result in no possibility of a drilling intrusion for the first 100 yr after the decommissioning of the WIPP (Chapt. 7, Ref. 10), and passive institutional controls are assumed to reduce the base drilling rate by two orders of magnitude between 100 and 700 yrs after decommissioning.[11]

For the computational implementation of the 1996 WIPP PA, it is convenient to represent the Poisson process for drilling intrusions by its corresponding rate term $\lambda_d(t)$ for intrusions into the area marked by the berm. Specifically,

$$\lambda_d(t) = 0 \text{ yr}^{-1} \qquad \text{for } 0 \leq t \leq 100 \text{ yr} \tag{3}$$

$$= (0.01)\,(0.6285 \text{ km}^2)\,(46.8/\text{km}^2/10^4 \text{ yr}) = 2.94 \times 10^{-5} \text{ yr}^{-1} \tag{4}$$

$$\text{for } 100 < t \leq 700 \text{ yr}$$

$$= (0.6285 \text{ km}^2)\,(46.8/\text{km}^2/10^4 \text{ yr}) = 2.94 \times 10^{-3} \text{ yr}^{-1} \tag{5}$$

$$\text{for } 700 < t \leq 10000 \text{ yr}$$

where 0.6285 km^2 is the area of the berm[12] and t is elapsed time since decommissioning of the WIPP.

The function $\lambda_d(t)$ defines the part of the probability space $(S_{st}, \mathcal{S}_{st}, p_{st})$ that corresponds to t_i. In the computational implementation of the analysis, $\lambda_d(t)$ is used to define the distribution of time between drilling intrusions (Fig. 2). As a reminder, the occurrence of one event in a Poisson process has no effect on the occurrence of the next event. Thus, the cumulative distributions in Fig. 2 can be used to define the time from one drilling event to the next (see Sect. 10). Due to the 10,000 yr regulatory period specified in 40 CFR 191.13, t_i is assumed to be bounded above by 10,000 yr in the definition of S_{st}. Further, t_i is assumed to be bounded below by 0 yr, although drilling intrusions prior to 100 yr cannot occur with $\lambda_d(t)$ as defined in Eqs. (3) - (5).

The function $\lambda_d(t)$ also determines the probability $prob(nBH = n|[a, b])$ that a future will have exactly n drilling intrusions in the time interval $[a, b]$ (Ref. 13), where

$$prob(nBH = n|[a, b]) = \left[\left(\int_a^b \lambda_d(t)dt\right)^n / n!\right] \exp\left(-\int_a^b \lambda_d(t)dt\right). \tag{6}$$

Further, the probability $prob(nBH \geq n \,|[a, b])$ that a future will have greater than or equal to n drilling intrusions in the time interval $[a, b]$ is given by

$$\begin{aligned} prob(nBH \geq n|[a,b]) &= 1 && \text{for } n = 0 \\ &= 1 - \sum_{m=0}^{n-1} prob(nBH = m|[a,b] && \text{for } n > 0. \end{aligned} \tag{7}$$

Example probabilities for drilling intrusions within the berm (i.e., for $\lambda_d(t)$ as defined in Eqs. (3) - (5)) and also for drilling intrusions into the nonexcavated and excavated areas beneath the berm are given in Table 1. The excavated area beneath the berm corresponds to the area in which waste disposal takes place.

3. Drilling Location l_i

Drilling locations are discretized to the 144 locations in Fig. 1. Given that a drilling intrusion occurs within the berm, it is assumed to be equally likely to occur at each of these 144 locations. Thus, the (conditional) probability pL_j that drilling intrusion i will occur at location L_j, $j = 1, 2, \ldots, 144$, in Fig. 1 is

$$pL_j = 1/144 = 6.94 \times 10^{-3}. \tag{8}$$

The probabilities pL_j define the part of $(S_{st}, \mathcal{S}_{st}, p_{st})$ associated with l_i.

4. Penetration of Excavated/Nonexcavated Area e_i

The variable e_i is a designator for whether or not the i^{th} drilling intrusion penetrates an excavated area of the repository (i.e., e_i = 0, 1 implies penetration of nonexcavated, excavated area, respectively). The corresponding probabilities pE_0 and pE_1 for $e_i = 0$ and $e_i = 1$ are

$$pE_1 = 0.1314 \text{ km}^2/0.6285 \text{ km}^2 = 0.209 \tag{9}$$

$$pE_0 = 1 - pE_1 = 0.791, \tag{10}$$

where 0.1314 km^2 and 0.6285 km^2 are the excavated area of the repository (Vol. 3, Ref. 14) and the area of the berm[12], respectively. The probabilities pE_0 and pE_1 define the part of $(\mathcal{S}_{st}, \mathcal{S}_{st}, p_{st})$ associated with e_i. The probabilities of different numbers of drilling intrusions into excavated and nonexcavated areas beneath the berm are illustrated in Table 1.

5. Penetration of Pressurized Brine b_i

The variable b_i is a designator for whether or not the i^{th} drilling intrusion penetrates pressurized brine (i.e., b_i = 0, 1 implies nonpenetration, penetration of pressurized brine). The corresponding probabilities pB_0 and pB_1 for b_i = 0 and $b_i = 1$ are 0.92 and 0.08, respectively.[15] The rationale for defining the probability of penetrating pressurized brine for individual drilling intrusions is based on the belief that the fractures in the Castile Formation that are capable of supplying significant quantities of brine are a small fraction (i.e., 0.08) of the area encompassed by the berm.[15] The probabilities pB_0 and pB_1 define the part of $(\mathcal{S}_{st}, \mathcal{S}_{st}, p_{st})$ that corresponds to b_i.

Example probabilities for futures with different numbers of drilling intrusions that penetrate pressurized brine within the berm (Fig. 1) and also within the nonexcavated and excavated areas beneath the berm are given in Table 2. The defining equations for these probabilities are the same as those in Eqs. (6) and (7) with $\lambda_d(t)$ replaced by the appropriate drilling rate into pressurized brine. In particular, these rates are the original drilling rates (i.e., the rates used in the generation of Table 1) multiplied by 0.08.

6. Plugging Pattern p_i

Three plugging patterns are considered in the 1996 WIPP PA: (1) p_1, which corresponds to a full concrete plug through Salado Formation to Bell Canyon Formation with a permeability of 5×10^{-17} m^2, (2) p_2, which corresponds to a two-plug configuration with concrete plugs at Rustler/Salado interface and Castile/Bell Canyon interface, and (3) p_3, which corresponds to a three-plug configuration with concrete plugs at Rustler/Salado, Salado/Castile and Castile/Bell Canyon interfaces (Ref. 16; App. DEL, Ref. 10). The probability that a given drilling intrusion will be sealed with plugging pattern p_j, $j = 1, 2, 3$, is given by pPL_j, where $pPL_1 = 0.02$, $pPL_2 = 0.68$ and $pPL_3 = 0.30$ (App. DEL, Ref. 10). The probabilities pPL_j define the part of $(S_{st}, \mathcal{S}_{st}, p_{st})$ that corresponds to p_j.

7. Activity Level $\mathbf{a}_i$

The waste intended for disposal at the WIPP is divided in 570 distinct waste streams (Table 3), with 569 of these waste streams designated as contact handled (CH)-TRU waste and one waste stream designated as remote handled (RH)-TRU waste. Each waste drum emplaced at the WIPP will contain waste from a single CH-TRU stream. Given that the CH-TRU drums will be stacked three high, each drilling intrusion through CH-TRU waste will intersect three waste streams. In contrast, there is only one waste stream for RH-TRU waste, and so each drilling intrusion through RH-TRU waste will intersect this single waste stream.

The concentrations and conditional probabilities for individual CH-TRU streams are indicated in Table 3. However, the large number of waste streams makes a complete display of this information cumbersome. A more compact summary of the probabilities and concentrations for the CH-TRU streams is provided by CCDFs for concentration at individual times (Fig. 3). Each CCDF in Fig. 3 summarizes the probability and concentration data indicated in Table 3 for CH-TRU waste at a specific time (i.e., 100, 125, …, 10,000 yr).

The vector $\mathbf{a}_i$ characterizes the type of waste penetrated by the i^{th} drilling intrusion. Specifically,

$$\mathbf{a}_i = a_i = 0 \tag{11}$$

if $e_i = 0$ (i.e., if the i^{th} drilling intrusion does not penetrate an excavated area of the repository);

$$\mathbf{a}_i = a_i = 1 \tag{12}$$

if $e_i = 1$ and RH-TRU is penetrated; and

$$\mathbf{a}_i = \left[2, \mathrm{CH}_{i1}, \mathrm{CH}_{i2}, \mathrm{CH}_{i3}\right] \tag{13}$$

if $e_i = 1$ and CH-TRU is penetrated, where CH_{i1}, CH_{i2} and CH_{i3} are designators for the CH-TRU waste streams intersected by the i^{th} drilling intrusion (i.e., each of CH_{i1}, CH_{i2} and CH_{i3} is an integer between 1 and 569).

Whether the i^{th} intrusion penetrates a nonexcavated or excavated area is determined by the probabilities pE_0 and pE_1 discussed in Sect. 4. Given that the i^{th} intrusion penetrates an excavated area, the probabilities pCH and pRH of penetrating CH- and RH-TRU waste are given by

$$pCH = aCH / aEX = \left(1.156 \times 10^5 \text{ m}^2\right) / \left(1.314 \times 10^5 \text{ m}^2\right) = 0.880 \tag{14}$$

$$pRH = aRH / aEX = \left(1.576 \times 10^4 \text{ m}^2\right) / \left(1.314 \times 10^5 \text{ m}^2\right) = 0.120, \quad (15)$$

where aCH is the excavated area used for disposal of CH-TRU waste (i.e., 1.576×10^5 m^2, which is the sum of a seal area of 4.133×10^3 m^2 and a waste disposal area of 1.115×10^5 m^2), aRH is the excavated area used for disposal of RH-TRU waste (i.e., 1.576×10^4 m^2), and $aEX = aCH + aRH$ (i.e., 1.314×10^5 m^2) (Vol. 3, Ref. 14).

As indicated in this section, the probabilistic characterization of $\mathbf{a}_i$ in $(S_{st}, \mathcal{S}_{st}, p_{st})$ depends on a number of individual probabilities. Specifically, pE_0 and pE_1 determine whether a nonexcavated or excavated area is penetrated (Sect. 4); pCH and pRH determine whether CH- or RH-TRU waste is encountered given penetration of an excavated area; and the individual waste stream probabilities in Table 3 (i.e., pCH_j, $j = 1, 2, \ldots, 569$) determine the waste streams encountered given a penetration of CH-TRU waste.

8. Mining Time t_{min}

Consistent with guidance in 40 CFR 194, full mining of known potash reserves within the land withdrawal boundary is assumed to occur at time t_{min}. In 40 CFR 194 (Ref. 19), the occurrence of mining within the land withdrawal boundary in the absence of institutional controls is specified as following a Poisson process with a rate of $\lambda_m = 1 \times 10^{-4}$ yr^{-1}. However, this rate can be reduced by active and passive institutional controls. Specifically, active institutional controls are assumed to result in no possibility of mining for the first 100 yr after decommissioning of the WIPP (Chapt. 7, Ref. 10), and passive institutional controls are assumed to reduce the base mining rate by two orders of magnitude between 100 and 700 yr after decommissioning.[11]

The preceding requirements lead to a time-dependent mining rate $\lambda_m(t)$. Specifically,

$$\lambda_m(t) = 0 \text{ yr}^{-1} \qquad \text{for } 0 \le t \le 100 \text{ yr} \quad (16)$$

$$= (0.01)\left(1 \times 10^{-4} \text{ yr}^{-1}\right) = 1 \times 10^{-6} \text{ yr}^{-1} \qquad \text{for } 100 < t \le 700 \text{ yr} \quad (17)$$

$$= 1 \times 10^{-4} \text{ yr}^{-1}, \qquad \text{for } 700 < t \le 10000 \text{ yr} \quad (18)$$

where t is elapsed time since decommissioning of the WIPP. The function $\lambda_m(t)$ defines the part of $(S_{st}, \mathcal{S}_{st}, p_{st})$ that corresponds to t_{min}. In the computational implementation of the analysis, $\lambda_m(t)$ is used to define the distribution of time to mining (Fig. 4). The use of $\lambda_m(t)$ to characterize t_{min} is analogous to the use of λ_d to characterize the t_i except that only one mining event is assumed to occur (i.e., $\mathbf{x}_{st}$ contains only one value for t_{min}) in consistency with guidance given in 40 CFR 194 that mining within the land withdrawal boundary should be assumed to remove all economically viable potash reserves. Due to the 10,000 yr regulatory period specified in 40 CFR 191.13, t_{min} is assumed to be bounded above by 10,000 yr in the definition of S_{st}. Further, t_{min} is assumed to be bounded below by 100 yr, although mining cannot occur prior to 100 yr with $\lambda_m(t)$ as defined in Eqs. (16) - (18).

9. Sampling Procedures

Extensive use is made of sampling procedures in the 1996 WIPP PA. In particular, random sampling is used in the generation of individual CCDFs (i.e., for integration over the probability space $(\mathcal{S}_{st}, \mathbb{S}_{st}, p_{st})$ for stochastic uncertainty; see Sect. 4, Ref. 1) and Latin hypercube sampling is used for the assessment of the effects of imprecisely known analysis inputs (i.e., for integration over the probability space $(\mathcal{S}_{su}, \mathbb{S}_{su}, p_{su})$ for subjective uncertainty; see Sect. 5, Ref. 1). Due to the importance of sampling procedures in the 1996 WIPP PA, brief descriptions are given for random sampling, importance sampling and Latin hypercube sampling. For notational convenience, the variable under consideration is represented by

$$\mathbf{x} = [x_1, x_2, ..., x_{nV}] \tag{19}$$

and the corresponding probability space is $(\mathcal{S}, \mathbb{S}, p)$.

In random sampling, the observations

$$\mathbf{x}_k = [x_{k1}, x_{k2}, ..., x_{k,nV}], \; k = 1, 2, ..., nR, \tag{20}$$

in a sample of size nR are selected according to the joint probability distribution for the elements of $\mathbf{x}$ as defined by $(\mathcal{S}, \mathbb{S}, p)$. In practice, $(\mathcal{S}, \mathbb{S}, p)$ is defined by specifying a distribution D_j for each element x_j of $\mathbf{x}$. Points from different regions of the sample space $\mathcal{S}$ occur in direct relationship to the probability of occurrence of these regions, and each sample element is selected independently of all other sample elements. As illustrated in Fig. 5 for $x_1 = U$, $x_2 = V$, $nV = 2$ and $nR = 5$, the numbers $RU(1)$, $RU(2)$, ..., $RU(5)$ are sampled from a uniform distribution on [0, 1] and in turn lead to a sample $U(1)$, $U(2)$, ..., $U(5)$ from U based on the cumulative distribution function (CDF) for U. Similarly, the numbers $RV(1)$, $RV(2)$, ..., $RV(5)$ lead to a sample $V(1)$, $V(2)$, ..., $V(5)$ from V. The pairs

$$\mathbf{x}_k = [U(k), V(k)], \; k = 1, 2, ..., nR = 5, \tag{21}$$

then constitute a random sample from $\mathbf{x} = [U, V]$. Random samples are generated in an analogous manner when $\mathbf{x}$ has a dimensionality greater than 2 (e.g., $nV = 50$).

With importance sampling, $\mathcal{S}$ is exhaustively divided into a number of nonoverlapping subregions (i.e., strata) $\mathcal{S}_i$, $i = 1, 2, ..., nS$. Then, nS_i values for $\mathbf{x}$ are randomly sampled from $\mathcal{S}_i$, with the random sampling carried out in consistency with the definition of $(\mathcal{S}, \mathbb{S}, p)$ and the restriction of $\mathbf{x}$ to $\mathcal{S}_i$. The resultant vectors

$$\mathbf{x}_k = [x_{k1}, x_{k2}, ..., x_{k,nV}], \; k = 1, 2, ..., \sum_{i=1}^{nS} nS_i \,, \tag{22}$$

then constitute an importance sample from S. Typically, only one value is sampled from each S_i. Importance sampling is used to assure the inclusion in an analysis of subsets of S that have high consequences but low probabilities.

Importance sampling operates to ensure the inclusion of specified regions in the sample space. This idea is carried farther in Latin hypercube sampling[20] to ensure the inclusion of the full range of each variable. Specifically, the range of each variable (i.e., the x_j) is divided into *nLHS* intervals of equal probability and one value is selected at random from each interval. The *nLHS* values thus obtained for x_1 are paired at random without replacement with the *nLHS* values obtained for x_2. These *nLHS* pairs are combined in a random manner without replacement with the *nLHS* values of x_3 to form *nLHS* triples. This process is continued until a set of *nLHS* nV-tuples is formed. These nV-tuples are of the form

$$\mathbf{x}_k = [x_{k1}, x_{k2}, ..., x_{k,nV}],\ k = 1, ..., nLHS, \tag{23}$$

and constitute the Latin hypercube sample (LHS). The individual x_j must be independent for the preceding construction procedure to work; a method for generating Latin hypercube and random samples from correlated variables has been developed by Iman and Conover[21]. Latin hypercube sampling is an extension of quota sampling[22] and can be viewed as an n-dimensional randomized generalization of Latin square sampling (pp. 206-209, Ref. 23).

The generation of an LHS of size $nLHS = 5$ from $\mathbf{x} = [U, V]$ is illustrated in Fig. 6. Initially, the ranges of U and V are subdivided into five intervals of equal probability, with this subdivision represented by the lines that originate at 0.2, 0.4, 0.6 and 0.8 on the ordinates of the two frames in Fig. 6, extend horizontally to the CDFs, and then drop vertically to the abscissas to produce the 5 indicated intervals. Random values $U(1)$, $U(2)$, ..., $U(5)$ and $V(1)$, $V(2)$, ..., $V(5)$ are then sampled from these intervals. The sampling of these random values is implemented by (1) sampling $RU(1)$ and $RV(1)$ from a uniform distribution on [0, 0.2], $RU(2)$ and $RV(2)$ from a uniform distribution on [0.2, 0.4], and so on and (2) then using the CDFs to identify (i.e., sample) the corresponding U and V values, with this identification represented by the dashed lines that originate on the ordinates of the two frames in Fig. 6, extend horizontally to the CDFs, and then drop vertically to the abscissas to produce $U(1)$, $U(2)$, ..., $U(5)$ and $V(1)$, $V(2)$, ..., $V(5)$. The generation of the LHS is then completed by randomly pairing (without replacement) the resulting values for U and V. As this pairing is not unique, many possible LHSs can result. For example, one LHS results from the pairings $[U(1), V(5)]$, $[U(2), V(1)]$, $[U(3), V(2)]$, $[U(4), V(3)]$, $[U(5), V(4)]$, and a different LHS results from the pairings $[U(1), V(3)]$, $[U(2), V(2)]$, $[U(3), V(3)]$, $[U(4), V(5)]$, $[U(5), V(1)]$. The generation of an LHS for $nV > 2$ proceeds in a similar manner.

Random sampling is the preferred technique when sufficiently large samples are possible because it is easy to implement, easy to explain, and provides unbiased estimates for means, variances and distribution functions. When the models under consideration are expensive to evaluate or estimates of extreme quantiles are needed, the required sample size to achieve a specific purpose could be too large to be computationally practicable. In the 1996 WIPP PA, random sampling is used for the estimation of CCDFs (i.e., integration over (S_{st}, $\mathcal{S}_{st}$, p_{st})) because it was possible to develop a computational strategy that allowed the use of a sample of size nS = 10,000 to estimate an exceedance probability of 0.001 (i.e., the 0.999 quantile of the distribution of normalized releases to the accessible environment).

When random sampling is not computationally feasible, importance sampling is often employed. For example, the fault and event tree techniques used in probabilistic risk assessments for nuclear power stations and other complex engineered facilities are algorithms for defining importance sampling procedures. However, the use of importance sampling on nontrivial problems is not easy due to the difficulty of both defining the necessary strata and calculating the probabilities of these strata. Without extensive *a priori* knowledge, the strata are likely to be defined in an inappropriate manner, with the result that importance sampling can end up requiring more calculations than random sampling to calculate the same outcomes. For example, the numbers of strata in the importance sampling procedure used to estimate CCDFs in the 1991 and 1992 WIPP PAs (Ref. 24) greatly exceeds the size of the random samples used in the 1996 WIPP PA to estimate CCDFs. Importance sampling was not used in the 1996 WIPP PA.

Latin hypercube sampling is used when large samples are not computationally practicable and the estimation of very high quantiles is not required. The preceding is typically the case in uncertainty and sensitivity studies to assess the effects of subjective uncertainty. First, the models under consideration are often computationally demanding, with the result that the number of calculations that can be performed to support the analysis is necessarily limited. For example, the totality of the model calculations (i.e., BRAGFLO, NUTS, PANEL, GRASP_INV, SECOFL2D, SECOTP2D, CUTTINGS_S, BRAGFLO_DBR; see Sect. 4, Ref. 1 and also Refs. 25 - 29) in the 1996 WIPP PA is too extensive to permit the generation of 1000's of CCDFs in an uncertainty/sensitivity study to assess the effects of subjective uncertainty on compliance with 40 CFR 191.13. Second, the estimation of very high quantiles is generally not required in an analysis to assess the effects of subjective uncertainty. Typically, a 0.90 or 0.95 quantile is adequate to establish where the available information indicates a particular analysis outcome is likely to be located; in particular, a 0.99, 0.999 or 0.9999 quantile is usually not needed in assessing the effects of subjective uncertainty.

Desirable features of Latin hypercube sampling include unbiased estimates for means and distribution functions and dense stratification across the range of each sampled variable.[20] Uncertainty and sensitivity analysis results obtained with Latin hypercube sampling have been observed to be quite robust even when relatively small samples (i.e., $nLHS$ = 50 to 200) are used.[30-32] Further, Latin hypercube sampling can be shown to outperform random sampling for monotonic functions[20] and to asymptotically (i.e., for increasing sample sizes) outperform random sampling for arbitrary functions.[33]

The 1996 WIPP PA uses random sampling to determine the effects of stochastic uncertainty (i.e., to integrate over $(S_{st}, \mathcal{S}_{st}, p_{st})$ and Latin hypercube sampling to determine the effects of subjective uncertainty (i.e., to integrate over $(S_{su}, \mathcal{S}_{su}, p_{su})$). In particular, Latin hypercube sampling is felt to be the most appropriate procedure to use to meet the requirement in 40 CFR 194.34(b) that "Computational techniques, which draw random samples from across the entire range of the probability distributions developed pursuant to paragraph (b) of this section, shall be used in generating CCDFs and shall be documented in any compliance application."

10. Generation of Individual Futures

A description follows for the manner in which random sampling is used to generate elements $\mathbf{x}_{st}$ of S_{st} for use in the CCDF construction indicated in Eq. (2). The drilling rate λ_d is used to generate the times at which drilling intrusions occur. For a Poisson process with a constant λ_d (i.e., a stationary process), the cumulative distribution function (CDF) for the time Δt between the successive events is given by (p. 113, Ref. 34)

$$prob(t \le \Delta t) = 1 - \exp(-\lambda_d \Delta t). \tag{24}$$

A uniformly distributed random number is selected from [0, 1]. Then, solution of

$$r_1 = 1 - \exp(-\lambda_d t_1) \tag{25}$$

for t_1 gives the time of the first drilling intrusion (Fig. 2). If 100 yr of administrative control is assumed, then 100 yr would be added to the t_1 obtained in Eq. (24) to obtain the time of the first drilling intrusion. Selection of a second random number r_2 and solution of

$$r_2 = 1 - \exp(-\lambda_d \Delta t_1) \tag{26}$$

for Δt_1 gives the time interval between the first and second drilling intrusions, with the outcome that $t_2 = t_1 + \Delta t_1$. This process can be continued until a time t_{n+1} is generated that exceeds 10,000 yr. The times $t_1, t_2, \ldots, t_n$ then constitute the drilling times in $\mathbf{x}_{st}$ in Eq. (1). A detailed description of the algorithm for generating individual drilling intrusion times is given in Table 4. The mining time t_{min} is sampled in a similar manner. Additional uniformly distributed random numbers from [0, 1] are used to generate the elements $l_i, e_i, b_i, p_i, \mathbf{a}_i, i = 1, 2, \ldots, n$, of $\mathbf{x}_{st}$ from their assigned distributions (see Sects. 3-7). A detailed description of the algorithm for generating individual futures is given in Table 5.

The 1996 WIPP PA assumed that drilling intrusions within the berm used as part of the passive marker system (Fig. 1) and potash mining within the land withdrawal boundary (Fig. 3, Ref. 28) are the only events involved in the definition of $\mathbf{x}_{st}$ in Eq. (1) and hence in the definition of the sample space S_{st} for stochastic uncertainty. The inclusion of additional potential occurrences in the definition of $(S_{st}, \mathcal{S}_{st}, p_{st})$ presents no conceptual problem.

Such occurrences could be incorporated into the definition of $\mathbf{x}_{st}$ and their associated probabilities used in the sampling process described in the preceding paragraph. For example, if deemed sufficiently important to the calculation of normalized releases, climatic change could be incorporated into the definition of $\mathbf{x}_{st}$ and hence ($\mathcal{S}_{st}$, $\mathcal{\mathcal{S}}_{st}$, p_{st}).

The algorithm in Table 5 describes how random sampling was used to generate a single future $\mathbf{x}_{st}$ in the 1996 WIPP PA. For each LHS element $\mathbf{x}_{su,k}$, $k = 1, 2, \ldots, 300$, used in the analysis (Sect. 5, Ref. 1; Sect. 8, Ref. 35), $nS = 10{,}000$ individual futures

$$\mathbf{x}_{st,i} = [t_{i1}, l_{i1}, e_{i1}, b_{i1}, p_{i1}, \mathbf{a}_{i1}, t_{i2}, l_{i2}, e_{i2}, b_{i2}, p_{i2}, \mathbf{a}_{i2}, \ldots, t_{in}, l_{in}, e_{in}, b_{in}, p_{in}, \mathbf{a}_{in}, t_{i,min}], i = 1, 2, \ldots, nS = 10{,}000, \quad (27)$$

were randomly sampled and used in the construction of all CCDFs for that LHS element. A different random seed was used to initiate the sampling of $\mathbf{x}_{st}$ for each LHS element, with the result that each LHS element uses different values for $\mathbf{x}_{st}$ in CCDF construction. As 300 LHS elements are used in the analysis and 10,000 futures are sampled for each LHS element, the total number of futures $\mathbf{x}_{st}$ used in the analysis in CCDF construction is 3×10^6.

11. Construction of CCDFs

The 1996 WIPP PA uses the sampled futures $\mathbf{x}_{st,i}$ in Eq. (27) to construct CCDFs for many different quantities (e.g., cuttings and cavings releases, spallings releases, direct brine releases, ...). The CCDF construction process is the same for each quantity. For notational convenience, assume that the particular quantity under consideration can be represented by the function $f(\mathbf{x}_{st,i})$, with the result that 10,000 values

$$f(\mathbf{x}_{st,i}), i = 1, 2, \ldots, 10{,}000 \quad (28)$$

are available for use in CCDF construction. Formally, the resultant CCDF is defined by the expression in Eq. (2). In practice, the indicator function δ_R in Eq. (2) is not directly used and the desired CCDF is obtained after an appropriate ordering of the $f(\mathbf{x}_{st,i})$ (i.e., from smallest to largest or largest to smallest) as described below.

In concept, the easiest way to construct the desired CCDF is to order the $f(\mathbf{x}_{st,i})$ from smallest to largest and then directly construct the CCDF with a weight of 10^{-4} assigned to each $f(\mathbf{x}_{st,i})$ (Fig. 7). However, this approach is cumbersome because it requires the $f(\mathbf{x}_{st,i})$ to be sorted from smallest to largest and also results in 10,000 plot points for each CCDF. As an aside, the included and excluded points appear in Fig. 7 because a CCDF gives the probability of exceeding a value. In practice, CCDFs are usually plotted with the distinction between included and excluded points omitted and vertical lines added at the discontinuities associated with these points (Fig. 8).

The 1996 WIPP PA uses a binning procedure in CCDF construction to simplify sorting the individual $f(\mathbf{x}_{st,i})$ and to reduce the number of plot points. Specifically, the range of f is divided into intervals (i.e., bins) by the specified points

$$f_{min} = b_0 < b_1 < b_2 < \ldots < b_n = f_{max}, \tag{29}$$

where f_{min} is the minimum value of f to be plotted (typically 10^{-6} or 10^{-5} when an EPA normalized release is under consideration), f_{max} is the maximum value of f to be plotted (typically 100 when an EPA normalized release is under consideration), n is the number of bins in use, and the b_i are typically loguniformly placed with 20 values per order of magnitude. A counter nB_j is used for each interval $[b_{j-1}, b_j]$. All counters are initially set to zero. Then, as individual values $f(\mathbf{x}_{st,i})$ are generated, the counter nB_j is incremented by 1 when the inequality

$$b_{j-1} < f(\mathbf{x}_{st,i}) \le b_j \tag{30}$$

is satisfied. As an aside, the indicated procedure is dynamic in the 1996 WIPP PA in the sense that, if necessary, f_{max} will be increased in value so that the inequality $f(\mathbf{x}_{st,i}) < f_{max}$ will always be satisfied. Once the 10,000 values for $f(\mathbf{x}_{st,i})$ have been generated, a value of nB_j will exist for each interval $[b_{j-1}, b_j]$. The nB_j satisfy the inequality

$$\sum_{j=1}^{n} nB_j \le 10{,}000 \tag{31}$$

because some of the $f(\mathbf{x}_{st,i})$ may satisfy the inequality $f(\mathbf{x}_{st,i}) < f_{min}$.

The quotient

$$pB_j = nB_j / 10{,}000 \tag{32}$$

provides an approximation to the probability that $f(\mathbf{x}_{st})$ will have a value that falls in the interval $[b_{j-1}, b_j]$. The resultant CCDF is then defined by the points

$$(b_j, prob(\text{value} > b_j)) = (b_j, \sum_{k=j+1}^{n} pB_j) \tag{33}$$

for $j = 0, 1, 2, \ldots, n-1$, where $prob(\text{value} > b_j)$ is the probability that a value greater than b_j will occur (Fig. 9).

The omitted points in the CCDF in Fig. 9 produce plots that are hard to read. This is especially true when multiple CCDFs appear in a single plot frame. One possibility is to add vertical lines at the discontinuities as indicated in Fig. 9. However, this can also produce plots that are hard to read when multiple CCDFs appear in a single plot frame due to the running together of the horizontal components of individual CCDFs at the discretized probability levels (e.g., at integer multiples of 10^{-4}), which makes it difficult to follow a single CCDF in the plot. Further, in most situations a stairstep CCDF should converge to a continuous CCDF as additional points (i.e., elements $\mathbf{x}_{st}$ of S_{st}) are used in its construction. For the preceding reasons, the 1996 WIPP PA "smooths" its CCDFs by drawing diagonal lines from included point to included point (i.e., from the left end of one bin to the left end of the next bin; see Fig. 10).

When multiple CCDFs appear in a single plot, the bottom of the plot can become very congested as the individual CCDFs drop to zero on the abscissa. For this reason, the CCDFs for comparison with the EPA release limits presented as part of the 1996 WIPP PA stop at the largest observed consequence value (e.g., a point in the interval $[b_{n-3}, b_{n-2}]$ in Fig. 10 as illustrated in Fig. 11). Stopping at the largest consequence value rather than the left bin boundary of the bin that contains this value (e.g., b_{n-3} in Fig. 11) permits the CCDF to explicitly show the largest observed consequence. However, given that 20 bins per order of magnitude are in use, this convention has no significant effect on the appearance of the resultant CCDFs.

Due to the use of a sample size of 10,000 in the generation of CCDFs for comparison with the EPA release limits, the last nonzero exceedance probability in the resultant CCDFs is typically 10^{-4} (Fig. 12). Specifically, the left frame of Fig. 12 shows what the CCDFs would look like if the plots dropped to zero from the largest observed value, and the right frame in Fig. 12 shows what the same CCDFs would look like with the convention of stopping at the largest observed consequence value. The only difference in the CCDFs in the left and right frames of Fig. 12 are the vertical lines between exceedance probabilities of 10^{-4} and 10^{-5}, where 10^{-5} is being used as a surrogate for an exceedance probability of zero. As already indicated, the plotting convention in the right frame of Fig. 12 is used in the 1996 WIPP PA. The horizontal lines near the bottom of the CCDFs in Fig. 12 result when the largest observed consequence value is preceded by several unpopulated bins. Further, the appearance of these horizontal lines is accentuated by the discretized probability values (i.e., integer multiples of 10^{-4}), which results in horizontal sections of different CCDFs running together; this same pattern can be seen in Fig. 11.

In the 1996 WIPP PA, the sampling of individual futures (Sect. 10) and associated CCDF construction is carried out by the CCDFGF program.[36, 37]

12. Mechanistic Calculations

The computational strategy used in the 1996 WIPP PA was to perform calculations with the models used to estimate normalized releases to the accessible environment (Sect. 4, Ref. 1; Refs. 25 - 29) for selected elements of S_{st} (Table 6) and then to use the results of these calculations to determine the releases to the accessible environment for the large number (i.e., 10,000) of randomly sampled futures used in the estimation of individual CCDFs. The same set of mechanistic calculations was performed for each LHS element used to incorporate the effects of subjective uncertainty (Sect. 5, Ref. 1; Sect. 1, Ref. 35). The manner in which these calculations were used to construct releases for the randomly sampled elements $\mathbf{x}_{st,i}$ of S_{st} is described elsewhere: cuttings and cavings in Ref. 26, spallings in Ref. 26, direct brine release in Ref. 27, release to Culebra in Ref. 29, transport in Culebra in Ref. 28, and total release to accessible environment in Ref. 39.

Four categories of calculations are indicated in Table 6 as being performed with BRAGFLO (i.e., E0, E1, E2, E2E1). In turn, the calculations associated with these categories can be viewed as being performed for specific elements $\mathbf{x}_{st}$ of S_{st}. In particular, the E0 calculation is performed for

$$\mathbf{x}_{st,0} = \text{element of } S_{st} \text{ that corresponds to no drilling intrusions and no mining (Note: } \mathbf{x}_{st,0} \text{ as defined here is different from } \mathbf{x}_{st,0} \text{ in Eq. (4) of Ref. 1).} \quad (34)$$

Similarly, the E1 calculations are performed for

$$\mathbf{x}_{st,1} = [t_1 = 350 \text{ yr}, l_1, e_1 = 1, b_1 = 1, p_1 = 2, \mathbf{a}_1] \quad (35)$$

$$\mathbf{x}_{st,2} = [t_1 = 1000 \text{ yr}, l_1, e_1 = 1, b_1 = 1, p_1 = 2, \mathbf{a}_1], \quad (36)$$

where $t_1 = 350$, 1000 yr indicates the time of the drilling intrusion (Sect. 2), $e_1 = 1$ indicates that an excavated area of the repository is penetrated by the drilling intrusion (Sect. 4), $b_1 = 1$ indicates that pressurized brine is penetrated by the drilling intrusion (Sect. 5), $p_1 = 2$ indicates that plugging pattern 2 is used (Sect. 6), the absence of specific values for drilling location l_1 (Sect. 3) and activity level $\mathbf{a}_1$ (Sect. 7) indicates that exact values for these characteristics are not specified, and the absence of a value for mining time t_m (Sect. 8) indicates that mining does not take place.

Although drilling location l_1 is not specified in Eqs. (35) and (36), some specification is required for the BRAGFLO calculations. If equivalent grids were used in the definition of $\mathbf{x}_{st}$ (Fig. 1) and in the numerical solution of the partial differential equations on which BRAGFLO is based (Fig. 1, Ref. 25), the location of the drilling intrusion used in the BRAGFLO calculations could be specified as a specific value for l_1, which in turn would correspond to one of the 144 locations in Fig. 1 that are designated by l in the definition of $\mathbf{x}_{st}$. However, as these grids are not the same, a unique pairing between a value for l_1 and the location of the drilling intrusion used in the computational grid employed with BRAGFLO is not possible. The BRAGFLO computational grid divides the repository into a single lower (i.e., down dip) waste panel and a composite of the 9 upper (i.e., up dip) waste panels, with the drilling intrusion taking place through the center of the lower panel (Fig. 1, Ref. 25). Thus, in the context of the locations in Fig. 1 potentially indexed by l_1, the drilling intrusion takes place at a location in Panel 4, 5 or 10 (i.e., at a location in one of the three most down dip waste panels).

The E2 calculations with BRAGFLO are performed for

$$\mathbf{x}_{st,3} = [t_1 = 350 \text{ yr}, l_1, e_1 = 1, b_1 = 0, p_1 = 2, \mathbf{a}_1] \quad (37)$$

$$\mathbf{x}_{st,4} = [t_1 = 1000 \text{ yr}, l_1, e_1 = 1, b_1 = 0, p_1 = 2, \mathbf{a}_1], \quad (38)$$

with $\mathbf{x}_{st,3}$ and $\mathbf{x}_{st,4}$ the same as $\mathbf{x}_{st,1}$ and $\mathbf{x}_{st,2}$ in Eqs. (35) and (36) except for the absence of a penetration of pressurized brine (i.e., $b_1 = 0$ rather than $b_1 = 1$). As in the BRAGFLO calculations for $\mathbf{x}_{st,1}$ and $\mathbf{x}_{st,2}$, the computational implementation of the analysis assumes that the drilling intrusion takes place through the center of the lower waste panel (Fig. 1, Ref. 25).

The E2E1 calculations with BRAGFLO are performed for

$$\mathbf{x}_{st,5} = [t_1 = 800 \text{ yr}, l_1, e_1 = 1, b_1 = 0, p_1 = 2, \mathbf{a}_1, t_2 = 2000 \text{ yr}, l_2, e_2 = 1, b_2 = 1, p_2 = 2, \mathbf{a}_2]. \quad (39)$$

As for the E1 and E2 intrusions, the locations l_1 and l_2 of the drilling intrusions are assumed to correspond to the center of the lower waste panel (Fig. 1, Ref. 25), with the effects of the two drilling intrusions and their associated plugging patterns being implemented through assumptions involving the time-dependent behavior of borehole permeability (Table 17, Ref. 40).

Ten categories of calculations are indicated in Table 6 as being performed with CUTTINGS_S: (1) intrusion into lower waste panel in previously unintruded (i.e., E0 conditions) repository at 100, 350, 1000, 3000, 5000, 10,000 yr; (2) intrusion into upper waste panel in previously unintruded repository at 100, 350, 1000, 3000, 5000, 10,000 yr; (3) initial E1 intrusion at 350 yr followed by a second intrusion into the same waste panel at 550, 750, 2000, 4000 or 10,000 yr; (4) initial E1 intrusion at 350 yr followed by a second intrusion into a different waste panel at 550, 750, 2000, 4000 or 10,000 yr; (5) initial E1 intrusion at 1000 yr followed by a second intrusion into the same waste panel at 1200, 1400, 3000, 5000 or 10,000 yr; (6) initial E1 intrusion at 1000 yr followed by a second intrusion into a different waste panel at 1200, 1400, 3000, 5000 or 10,000 yr; (7) initial E2 intrusion at 350 yr followed by a second intrusion into the same waste panel at 550, 750, 2000, 4000 or 10,000 yr; (8) initial E2 intrusion at 350 yr followed by a second intrusion into a different waste panel at 550, 750, 2000, 4000 or 10,000 yr; (9) initial E2 intrusion at 1000 yr followed by a second intrusion into the same waste panel at 1200, 1400, 3000, 5000 or 10,000 yr; (10) initial E2 intrusion at 1000 yr followed by a second intrusion into a different waste panel at 1200, 1400, 3000, 5000 or 10,000 yr. Categories (1) and (2) involve elements $\mathbf{x}_{st}$ of S_{st} of the form

$$\mathbf{x}_{st,6} = [t_1, l_1, e_1 = 1, b_1, p_1, \mathbf{a}_1], \quad (40)$$

where t_1 = 100, 350, 1000, 3000, 5000 or 10,000 yr, l_1 corresponds to an intrusion into the lower waste panel (i.e., Panel 4, 5 or 10 in Fig. 1 and region 23 in Fig. 7, Ref. 25) for Category (1) and into the upper waste panels (i.e., Panel 1, 2, 3, 6, 7, 8 or 9 in Fig. 1 and region 24 in Fig. 7, Ref. 25) for Category (2), $e_i = 1$ indicates that the intrusion takes place into an excavated area of the repository, b_1 and p_1 are unspecified because these characteristics do not affect results calculated by CUTTINGS_S for use in the 1996 WIPP PA, and $\mathbf{a}_1$ corresponds to the penetration of CH-TRU waste (i.e., $\mathbf{a}_1$ = [2, CH_{11}, CH_{12}, CH_{13}], although only the property that CH-TRU waste is penetrated is used in the calculation with CUTTINGS_S). The characteristics specified by b_1 and p_1 (i.e., penetration of pressurized brine and plugging pattern) are not relevant to the determination of cuttings and spallings releases because these releases take place at the time that the drilling intrusion penetrates the repository. The penetration of CH-TRU waste is important because this determines the material properties used in the cavings and spallings calculations; the penetration of RH-TRU waste is assumed to result in no cavings and spallings releases. The actual locations at which the intrusions are assumed occur correspond to the points in Fig. 1 of Ref. 27 designated "Down-dip well, first or second intrusion" for Category (1) intrusions and "Up-dip well, first or second intrusion" for Category (2) intrusions. As described in conjunction with Fig. 2 of Ref. 27, pressures for use at the indicated points in Fig. 1 of Ref. 27 are obtained from calculations performed with BRAGFLO on the computational grid in Fig. 1 of Ref. 25.

Categories (3) - (6) for the calculations performed with CUTTINGS_S involve elements $\mathbf{x}_{st}$ of S_{st} of the form

$$\mathbf{x}_{st,7} = \left[t_1, l_1, e_1 = 1, b_1 = 1, p_1 = 2, \mathbf{a}_1, t_2, l_2, e_2 = 1, b_2, p_2, \mathbf{a}_2\right], \tag{41}$$

where t_1 = 350 yr for Categories (3) and (4), t_1 = 1000 yr for Categories (5) and (6), t_2 = 550, 750, 2000, 4000 and 10,000 yr for Categories (3) and (4), t_2 = 1200, 1400, 3000, 5000 and 10,000 yr for Categories (5) and (6), l_1 and l_2 correspond to intrusions into the same waste panel (Fig. 1) for Categories (3) and (5), l_1 and l_2 correspond to intrusions into different waste panels for Categories (4) and (6), $e_1 = e_2 = 1$ indicates that both intrusions take place into excavated areas of the repository, $b_1 = 1$ indicates that the first intrusion penetrates pressurized brine, $p_1 = 2$ indicates that plugging pattern 2 is used with the first intrusion, $\mathbf{a}_1$ and $\mathbf{a}_2$ correspond to the penetration of CH-TRU waste (i.e., $\mathbf{a}_i$ = [2, CH_{i1}, CH_{i2}, CH_{i3}], i = 1,2, although only the property that CH-TRU waste is penetrated is used in the calculation with CUTTINGS_S), and p_2 is unspecified. In the computational implementation of the analysis, intrusions into different waste panels are implemented by assuming that the first and second intrusions occur at the locations in Fig. 1 of Ref. 27 designated "Down-dip well, first or second intrusion" and "Up-dip well, first or second intrusion," respectively, and intrusions into the same waste panel are implemented by assuming that both intrusions occur at the location in Fig. 1 of Ref. 27 designated "Down-dip well, first or second intrusion." Thus, intrusions into different waste panels are implemented computationally as an initial intrusion into a lower (i.e., down dip) waste panel followed by a second intrusion into an upper (i.e., up dip) waste panel, and intrusions into the same waste panel are implemented computationally as two intrusions into the same lower (i.e., down dip) waste panel.

Categories (7) - (10) for the calculations performed with CUTTINGS_S involve elements $\mathbf{x}_{st}$ of S_{st} of the form

$$\mathbf{x}_{st,8} = [t_1, l_1, e_1 = 1, b_1 = 0, p_1 = 2, \mathbf{a}_1, t_2, l_2, e_2 = 1, b_2, p_2, \mathbf{a}_2]. \tag{42}$$

The vectors $\mathbf{x}_{st,8}$ associated with Categories (7) - (10) are the same as the vectors $\mathbf{x}_{st,7}$ associated with Categories (4) - (6) except for the use of $b_1 = 0$ instead of $b_1 = 1$, which implies that the first intrusion associated with $\mathbf{x}_{st,7}$ penetrates pressurized brine while the first intrusion associated with $\mathbf{x}_{st,8}$ does not penetrate pressurized brine.

As described in Ref. 26, the results obtained with CUTTINGS_S for the elements of S_{st} indicated in Eqs. (40) - (42) are then used in conjunction with algebraic procedures to construct releases due to cuttings and cavings and also due to spallings for arbitrary elements $\mathbf{x}_{st}$ of S_{st} sampled in the Monte Carlo construction of CCDFs for comparison with the boundary line specified in 40 CFR 191.13.

Calculations are performed for BRAGFLO_DBR for the same ten categories as for CUTTINGS_S (Table 6). Thus, the elements of S_{st} in Eqs. (40) - (42) also characterize the elements of S_{st} for which BRAGFLO_DBR calculations are performed. Further, BRAGFLO_DBR also uses the spallings releases calculated by CUTTINGS_S for these elements of S_{st} as input Ref. 27. As described in Ref. 27, the results obtained with BRAGFLO_DBR are then used in conjunction with algebraic procedures to construct direct brine releases for arbitrary elements $\mathbf{x}_{st}$ of S_{st} sampled in the Monte Carlo construction of CCDFs for comparison with the boundary line specified in 40 CFR 191.13.

Three categories of calculations are indicated in Table 6 as being performed with NUTS (i.e., E0, E1, E2). The E0 calculation is performed for the vector $\mathbf{x}_{st,0}$ in Eq. (41). The E1 calculations are performed for vectors of the form appearing in Eqs. (35) and (36) with t_1 = 100, 350, 1000, 3000, 5000, 7000 and 9000 yr. Similarly, the E2 calculations are performed for vectors of the form appearing in Eqs. (37) and (38) with t_1 = 100, 350, 1000, 3000, 5000, 7000 and 9000 yr. The BRAGFLO flow fields calculated for intrusions at 350 yr are moved back in time to 100 yr to support the NUTS calculations for t_1 = 100 yr; similarly, the BRAGFLO flow fields calculated for intrusions at 1000 yr are moved forward in time to support the NUTS calculations for t_1 = 3000, 5000, 7000 and 9000 yr.

One category of calculations is indicated in Table 6 as being performed with PANEL (i.e., E2E1). The associated calculations are performed for vectors $\mathbf{x}_{st,5}$ of the form appearing in Eq. (46). The PANEL calculations are based on the E2E1 BRAGFLO calculation in which t_1 = 800 yr and t_2 = 2000 yr in $\mathbf{x}_{st,5}$. The PANEL calculations are for t_2 = 100, 350, 1000, 2000, 4000, 6000 and 9000 yr in $\mathbf{x}_{st,5}$. The single BRAGFLO calculation for $\mathbf{x}_{st,5}$ as defined in Eq. (39) supports the PANEL calculations by having the flow fields calculated by BRAGFLO moved forward or backward in time as appropriate to match the value for t_2 in the PANEL calculations. In concept, this can be viewed as having the corresponding values for t_1 in $\mathbf{x}_{st,5}$ for the PANEL calculations assigned values of

$$t_1 = \max\{100\ \text{yr}, t_2 - 1200\ \text{yr}\}, \quad (43)$$

where the restriction that t_1 cannot be less than 100 yr results because the definition of $\mathbf{x}_{st}$ does not allow negative intrusion times and the assumption of 100 yr of administrative control (i.e., $\lambda_d(t) = 0\ \text{yr}^{-1}$ for $0 \le t \le 100$ yr; see Eq. (3)) results in a probability of zero for intrusion times between 0 and 100 yr. Under this convention, what is specified in concept by the definition of $\mathbf{x}_{st,5}$ for the PANEL calculations differs from what is actually done computationally because t_1 does indeed precede t_2 by 1200 yr in the BRAGFLO calculation.

As described in Ref. 29, the results obtained with NUTS and PANEL for elements of S_{st} of the form indicated in Eqs. (34) - (39) are then used in conjunction with algebraic procedures to construct time-dependent releases to the Culebra for arbitrary elements $\mathbf{x}_{st}$ of S_{st} sampled in the Monte Carlo construction of CCDFs for comparison with the boundary line specified in 40 CFR 191.13.

The SECOFL2D calculations are performed for two categories of conditions (Table 6): partially mined conditions in the vicinity of the repository (Fig. 1, Ref. 28) and fully mined conditions in the vicinity of the repository (Fig. 2, Ref. 28). As a reminder, partially mined conditions are assumed to always exist by the end of the period of administrative control (i.e., at 100 yr) in assessing compliance with 40 CFR 191.13 (Refs. 19, 41). The SECOFL2D calculations for partially mined conditions are performed for the element $\mathbf{x}_{st,0}$ of S_{st} defined in Eq. (34). The SECOFL2D calculations for fully mined conditions are performed for the element $\mathbf{x}_{st,m}$ of S_{st} given by

$$\mathbf{x}_{st,m} = [t_{min} = 100\ \text{yr}], \quad (44)$$

which corresponds to the future in which no drilling intrusion occurs and full mining occurs at $t_{min} = 100$ yr.

The SECOTP2D calculations are performed for the same two categories of conditions as the SECOFL2D calculations (Table 6). Thus, the SECOTP2D calculations are performed for the elements $\mathbf{x}_{st,0}$ and $\mathbf{x}_{st,m}$ of S_{st} defined in Eqs. (34) and (44), with the flow fields required in these calculations supplied by the calculations with SECOFL2D for $\mathbf{x}_{st,0}$ and $\mathbf{x}_{st,m}$. As described in Ref. 28, the results obtained for $\mathbf{x}_{st,0}$ and $\mathbf{x}_{st,m}$ with SECOTP2D are then used in conjunction with algebraic procedures to construct Culebra transport results for arbitrary elements $\mathbf{x}_{st}$ of S_{st} sampled in the Monte Carlo construction of CCDFs for comparison with the boundary line specified in 40 CFR 191.13.

13. Kaplan/Garrick Ordered Triple Representation for Risk

The 1991 and 1992 WIPP PAs (Refs. 14, 42) used the Kaplan and Garrick[5] ordered triple representation for risk as a basis for CCDF construction.[24] In this representation, risk is characterized by a set R of the form

$$R = \{(S_j, pS_j, \mathbf{cS}_j), j = 1, 2, \ldots, nS\}, \quad (45)$$

where S_j is a subset of the sample space S_{st} for stochastic uncertainty (i.e., an element of $\mathcal{S}_{st}$), the S_j have no futures in common (i.e., $S_j \cap S_k = \varnothing$ if $j \neq k$), the S_j are all inclusive in the sense that $S_{st} = \cup_j S_j$, pS_j is the probability of S_j (i.e., $pS_j = p_{st}(S_j)$), $\mathbf{cS}_j$ is a vector of consequence values associated with S_j (e.g., one of the many elements cS_j of $\mathbf{cS}_j$ would be the EPA normalized release specified in 40 CFR 191.13(a)), and nS is the number of sets (i.e., scenarios) into which S_{st} is decomposed. The construction of a CCDF for a particular consequence contained in $\mathbf{cS}$ proceeds in exactly the same manner as described in Figs. 7 - 10 except that each consequence value cS_j has a probability of pS_j rather than a fixed probability as is the case when random sampling is used to select the futures for which consequence results will be calculated (e.g., a probability of 10^{-4} when a sample of size 10,000 is used). As an aside, it is technically incorrect to refer to probabilities for elements of random samples. These numbers (i.e., probabilities) are actually weights that are used in estimating distributions and related quantities; the individual sample elements typically have probabilities of zero.

The 1991 and 1992 WIPP PAs used an importance sampling procedure to subdivide S_{st} into the sets S_j, to determine the probabilities pS_j, and to calculate the consequences in $\mathbf{cS}_j$.[13, 24] By the 1996 WIPP PA, the elements $\mathbf{x}_{st}$ of S_{st} had become too complex to be amendable to the use of an importance sampling procedure (see Sect. 13). Therefore, the PA switched to a Monte Carlo procedure (i.e., simple random sampling; see Ref. 43) for integration over S_{st} to produce the CCDF specified in 40 CFR 191.13(a). However, it is still possible to express the results in the Kaplan/Garrick representation in Eq. (45) by appropriately defining the sets S_j in terms of the bin boundaries b_j, $j = 0, 1, 2, \ldots, n$, in Eq. (46). Specifically, the sets $S_0, S_1, S_2, \ldots, S_n$ are defined by

$$S_0 = \{\mathbf{x}_{st}: f(\mathbf{x}_{st}) \leq b_0\} \tag{46}$$

and

$$S_j = \{\mathbf{x}_{st}: b_{j-1} < f(\mathbf{x}_{st}) \leq b_j\}, j = 1, 2, \ldots, n, \tag{47}$$

where $f(\mathbf{x}_{st})$ is the normalized release associated with $\mathbf{x}_{st}$. The sets $S_0, S_1, S_2, \ldots, S_n$ in Eqs. (46) and (47) correspond to the sets S_j, $j = 1, 2, \ldots, nS$, in Eq. (45). Further, approximations to the probabilities of these sets are given by

$$pS_j = p_{st}(S_j) \doteq pB_j, j = 1, 2, \ldots, n, \tag{48}$$

and

$$pS_0 = p_{st}(S_0) \doteq 1 - \sum_{j=1}^{n} pB_j, \tag{49}$$

where pB_j is defined in Eq. (32). Finally, the sets S_j are assigned the consequence

$$cS_0 = 0 \text{ and } cS_j = b_{j-1}, j = 1, 2, \ldots, n. \tag{50}$$

The preceding assignments for S_j, pS_j and cS_j in the definition of the set R in Eq. (45) results in the same CCDF as the construction procedure used in the 1996 WIPP PA and described in conjunction with Figs. 10 and 11.

Although the procedure for CCDF construction used in the 1996 WIPP PA and the procedure used in the 1991 and 1992 WIPP PAs can both be formally represented in terms of the Kaplan/Garrick representation for risk, there is an underlying difference in approach. The 1991 and 1992 PAs defined the sets S_j entirely on the basis of properties of $\mathbf{x}_{st}$. This approach has already been referred to as a form of importance sampling because of the division of S_{st} into sets and the assignment of probabilities to these sets. However, it can also be viewed as an integration problem in the spirit of the Riemann integral in the sense that it is based on laying a systematic grid on the space that is being integrated over (i.e., S_{st}). The 1996 WIPP PA defined the sets S_j on the basis of the values assumed by $f(\mathbf{x}_{st})$, which results in the possibility that a given set S_j will contain elements $\mathbf{x}_{st}$ from very different regions of S_{st}. This can also be viewed as an integration problem, but it is now an integration problem in the spirit of the Lebesgue integral, as sets based on the range of f rather than simply on a partitioning of S_{st} are under consideration (App. B, Ref. 44). In consistency with the concept of Lebesgue integration, the determination of pS_j can be viewed as the estimation of a probability measure (i.e., a probabilistic size) for S_j. However, when appropriately implemented, both approaches lead to approximations of the same CCDF.

The individual randomly sampled futures can also be used in the following expression with the same structure as the Kaplan/Garrick ordered triple representation for risk:

$$\mathrm{R} = \{(\mathbf{x}_{st,i}, 1/nS, \mathbf{f}(\mathbf{x}_{st,i})), i = 1, 2, \ldots, nS\}, \tag{51}$$

where nS = 10,000 in the 1996 WIPP PA and $\mathbf{f}(\mathbf{x}_{st,i})$ is a vector of consequence values associated with $\mathbf{x}_{st,i}$. Although the preceding representation leads to approximations of the same CCDFs as the representation in Eq. (45), the individual terms are different. Specifically, the S_j in Eq. (45) are disjoint sets such that $S_{st} = \cup_j S_j$; in contrast, the $\mathbf{x}_{st,i}$ in Eq. (51) are elements randomly sampled from S_{st} with $S_{st} \neq \cup_i\{\mathbf{x}_{st,i}\}$. The pS_j in Eq. (45) are the probabilities of the sets S_j; in contrast, $1/nS$ in Eq. (46) is a weight used in estimating CCDFs but is not equal to the probability of $\mathbf{x}_{st,i}$. The $\mathbf{cS}_j$ in Eq. (45) are representative of the consequences associated with S_j and, as such, might be calculated for a single representative element $\mathbf{x}_{st,j}$ of S_j or, more appropriately but very unlikely in practice, might be the expected consequences associated with S_j; in contrast, $\mathbf{f}(\mathbf{x}_{st,i})$ in Eq. (37) is calculated specifically for $\mathbf{x}_{st,i}$.

14. Scenarios and Scenario Probabilities

In the formal development of the 1996 WIPP PA, a scenario is a subset S of the sample space S_{st} for stochastic uncertainty. More specifically, a scenario is an element S of the set $\mathcal{S}_{st}$ in the probability space (S_{st}, $\mathcal{S}_{st}$, p_{st}) for stochastic uncertainty, and the probability of S is given by p_{st} (S). Thus, a scenario is what is called an event in the usual terminology of probability theory.

Given the complexity of the elements $\mathbf{x}_{st}$ of S_{st} (see Eq. (1)), infinitely many different scenarios can be defined. Several examples follow:

S_0 = {$\mathbf{x}_{st}$: $\mathbf{x}_{st}$ involves no drilling intrusion through an excavated area of the repository (i.e., $n = 0$ or $e_i = 0$ in Eq. (1) for $i = 1, 2, \ldots, n > 0$)} (52)

S_1 = {$\mathbf{x}_{st}$: $\mathbf{x}_{st}$ involves exactly one drilling intrusion through an excavated area of the repository, with this intrusion penetrating pressurized brine in the Castile Fm (i.e., $n > 0$ in Eq. (1) and there exists an integer i such that $1 \le i \le n$, $e_i = 1$, $b_i = 1$, and $e_j = 0$ for $j \ne i$ and $1 \le j \le n$)} (53)

S_2 = {$\mathbf{x}_{st}$: $\mathbf{x}_{st}$ involves exactly one drilling intrusion through an excavated area of the repository, with this intrusion not penetrating pressurized brine in the Castile Fm (i.e., $n > 0$ in Eq. (1) and there exists an integer i such that $1 \le i \le n$, $e_i = 1$, $b_i = 0$, and $e_j = 0$ for $j \ne i$ and $1 \le j \le n$)} (54)

S_3 = {$\mathbf{x}_{st}$: $\mathbf{x}_{st}$ involves exactly one drilling intrusion through an excavated area of the repository (i.e., $n > 0$ in Eq. (1) and there exists an integer i such that $1 \le i \le n$, $e_i = 1$, and $e_j = 0$ for $j \ne i$ and $1 \le j \le n$)}. (55)

The definitions of the preceding four scenarios are quite simple. In general, scenarios can be defined on the basis of any possible characterization of the properties of the individual elements of $\mathbf{x}_{st}$, which can lead to very complex scenario definitions.

The immediately preceding sentence implies that $\mathcal{S}_{st}$ can be defined to be all possible subsets of S_{st}. This is correct at an intuitive level and, for practical purposes, $\mathcal{S}_{st}$ can be thought of as containing all subsets of S_{st}. However, to obtain a mathematically rigorous development of probability (Sect. IV. 4, Ref. 45), $\mathcal{S}_{st}$ and p_{st} must have the following properties: (1) if $E \in \mathcal{S}_{st}$, then $E^c \in \mathcal{S}_{st}$, where the superscript c is used to denote the complement of E, (2) if $\{E_i\}$ is a countable collection of elements of $\mathcal{S}_{st}$, then $\cup_i E_i$ and $\cap_i E_i$ are also elements of $\mathcal{S}_{st}$, (3) $p_{st}(S_{st}) = 1$, (4) if $E \in \mathcal{S}_{st}$, then $0 \le p_{st}(E) \le 1$, and (5) if $E_1, E_2, \ldots$ is a sequence of disjoint sets from $\mathcal{S}_{st}$ (i.e., $E_i \cap E_j = \varnothing$ if $i \ne j$), then $p_{st}(\cup_i E_i) = \sum_i p_{st}(E_i)$. Properties (1) - (5) are describing characteristics that are intuitively expected of scenarios. Specifically, Property (1) implies that, if the occurrence of event E is a scenario, then the nonoccurrence of event E is also a scenario; Property (2) implies that, if the occurrence of each of the events $E_1, E_2, \ldots$ is a scenario, then the occurrence of E_1 or E_2 or … is a scenario, and similarly the occurrence of E_1 and E_2 and … is also a scenario, where the indicated sequence of scenarios (i.e., E_1, E_2, …) can be finite or infinite; Property (3) implies that the sample space S_{st} contains everything that could possibly occur (i.e., the sample space S_{st} is a scenario that has a probability of 1); Property (4) implies that all scenarios have probabilities between 0 and 1; and Property (5) implies that, if E_1, E_2, … is a sequence of mutually exclusive scenarios (i.e., E_i and E_j cannot both occur if $i \neq j$), then the probability of E_1 occurring or E_2 occurring or … is the sum of the probabilities for E_1, E_2, …, where the indicated sequence of scenarios can be finite or infinite. With considerable mathematical ingenuity, subsets of S_{st} can be constructed such that it is not possible to define a function p_{st} satisfying Properties (3) - (5) (Sect. 1.29, Ref. 46); thus, in a formal mathematical development, $\mathcal{S}_{st}$ cannot consist of all possible subsets of S_{st}. However, subsets of S_{st} that do not permit a suitable definition for p_{st} are so esoteric that their exclusion from $\mathcal{S}_{st}$ by the requirement that Properties (1) - (5) be satisfied does not result in the removal of any scenarios of potential interest in PA.

In the terminology of the 1996 WIPP PA, S_0 is typically called the E0 scenario (i.e., no drilling intrusions through the repository), S_1 is typically called the E1 scenario (i.e., a single drilling intrusion through the repository that penetrates pressurized brine), and S_2 is typically called the E2 scenario (i.e., a single drilling intrusion through the repository that does not penetrate pressurized brine). Another important scenario is defined by

$S_{21} = \{\mathbf{x}_{st}$: $\mathbf{x}_{st}$ involves exactly two drilling intrusions through excavated areas of the repository, with the first intrusion not penetrating pressurized brine and the second intrusion penetrating pressurized brine (i.e., $n \geq 2$ in Eq. (1) and there exist integers i, j such that $1 \leq i < j \leq n$, $e_i = 1$, $b_i = 0$, $e_j = 1$, $b_j = 1$, and $e_k = 0$ for $k \neq i, j$ and $1 \leq k \leq n)\}$ (56)

In the terminology of the 1996 WIPP PA, S_{21} is typically called the E2E1 scenario.

The scenarios S_0, S_1, S_2, S_3 and S_{21} are elements of $\mathcal{S}_{st}$, and their probabilities are formally represented by $p_{st}(S_0)$, $p_{st}(S_1)$, $p_{st}(S_2)$, $p_{st}(S_3)$, and $p_{st}(S_{21})$, with these probabilities deriving from the probability distributions assigned to the individual elements of $\mathbf{x}_{st}$. For example,

$$p_{st}(S_0) = \exp\left(-\int_a^b pE_1 \lambda_d(t)dt\right) = 3.27 \times 10^{-3} \quad (57)$$

$$p_{st}(S_1) = \left[\left(\int_a^b pE_1 \lambda_d(t)dt\right)^1 \Big/ 1!\right]\left[\exp\left(-\int_a^b pE_1 \lambda_d(t)dt\right)\right]\left[pB_1\right] = 1.50 \times 10^{-3} \quad (58)$$

$$p_{st}(S_2) = \left[\left(\int_a^b pE_1\lambda_d(t)dt\right)^1 \Big/ 1!\right]\left[\exp\left(-\int_a^b pE_1\lambda_d(t)dt\right)\right]\left[pB_0\right]$$

$$= 1.72 \times 10^{-2} \tag{59}$$

$$p_{st}(S_3) = \left[\left(\int_a^b pE_1\lambda_d(t)dt\right)^1 \Big/ 1!\right]\left[\exp\left(-\int_a^b pE_1\lambda_d(t)dt\right)\right]$$

$$= 1.87 \times 10^{-2}, \tag{60}$$

where $[a, b] = [0, 10{,}000 \text{ yr}]$, $pE_1 = 0.209$ (see Sect. 4), $pB_0 = 0.08$ (see Sect. 5), $pB_1 = 0.92$ (see Sect. 5), $\lambda_d(t)$ is defined in Eqs. (3) - (5), and the probabilities in Eqs. (57) - (60) are based on the relationship in Eq. (6).

The expressions defining $p_{st}(S_0)$, $p_{st}(S_1)$, $p_{st}(S_2)$ and $p_{st}(S_3)$ are relatively simple because the scenarios S_0, S_1, S_2 and S_3 are relatively simple. The scenario S_{21} is more complex and, as a result, $p_{st}(S_{21})$ is also more complex. Specifically,

$$\begin{aligned} p_{st}(S_{21}) &= \int_a^b p_{[a,t]}(nI=1, nB=0)[pB_1 pE_1\lambda_d(t)]p_{[t,b]}(nI=0)dt \\ &= \int_a^b\left[\int_a^t pB_0 pE_1\lambda_d(\tau)d\tau\right]\left[\exp\left(-\int_a^t pE_1\lambda_d(\tau)d\tau\right)\right]\left[pB_1 pE_1\lambda_d(t)\right]\left[\exp\left(-\int_t^b pE_1\lambda_d(\tau)d\tau\right)\right]dt \\ &= pB_0 pB_1 pE_1^2\left[\int_a^b\left(\int_a^t \lambda_d(\tau)d\tau\right)\lambda_d(t)dt\right]\left[\exp\left(-\int_a^b pE_1\lambda_d(t)dt\right)\right], \end{aligned} \tag{61}$$

where

$[a, b] = [0, 10{,}000 \text{ yr}]$

$p_{[a,t]}(nI = 1, nB = 0)$ = probability that exactly one intrusion (i.e., $nI = 1$) will penetrate an excavated area of the repository during the time interval $[a, t]$, with this intrusion not penetrating pressurized brine (i.e., $nB = 0$)

$$= \left[\left(\int_a^t pB_0 pE_1\lambda_d(\tau)d\tau\right)^1 \Big/ 1!\right]_1 \left[\exp\left(-\int_a^t pB_0 pE_1\lambda_d(\tau)d\tau\right)\right]_2 \left[\exp\left(-\int_a^t pB_1 pE_1\lambda_d(\tau)d\tau\right)\right]_3$$

$$= \left[\int_a^t pB_0 pE_1\lambda_d(\tau)d\tau\right]\left[\exp\left(-\int_a^t pE_1\lambda_d(\tau)d\tau\right)\right] \tag{62}$$

$p_{[t,\,b]}(nI = 0)$ = probability that no intrusions (i.e., nI = 0) will penetrate an excavated area of the repository during the time interval $[t, b]$

$$= \exp\left(-\int_t^b pE_1 \lambda_d(\tau)d\tau\right) \tag{63}$$

and the derivation of Eq. (61) generally follows the ideas in the derivation of Eq. (22) in Ref. 13. In the definition of $p_{[a,t]}(nI = 1, nB = 0)$ in Eq. (62), the product $[\sim]_1$ $[\sim]_2$ gives the probability that exactly one intrusion through an excavated area of the repository that does not penetrate pressurized brine will occur during the time interval $[a, t]$, and $[\sim]_3$ gives the probability that no intrusions that penetrate pressurized brine will occur during $[a, t]$.

More complex scenarios can be defined but with a corresponding increase in the complexity of the closed-form representation for scenario probability.[13] For example, consider the following relatively simple scenario:

S_4 = {$\mathbf{x}_{st}$: $\mathbf{x}_{st}$ involves exactly two drilling intrusions in the time interval $[a, b]$ and the mining event (i.e., t_{min}) also occurs in $[a, b]$, with the first drilling intrusion penetrating pressurized brine, using plugging pattern 2 and failing to penetrate an excavated area of the repository and the second drilling intrusion penetrating pressurized brine, an excavated area of the repository and RH waste and using plugging pattern 3 (i.e., $n \geq 2$ in Eq. (1), $a \leq t_{min} \leq b$, and there exists an integer i such that $1 \leq i < n$, $a \leq t_i \leq t_{i+1} \leq b$, $e_i = 0$, $b_i = 1$, $p_i = 2$, $\mathbf{a}_i = 0$, $e_{i+1} = 1$, $b_{i+1} = 1$, $p_{i+1} = 3$, $\mathbf{a}_{i+1} = 1$, and $t_k < a$ or $b < t_k$ for $k \neq i$, i+1 and $1 \leq k \leq n$)} (64)

The corresponding probability is given by

$$\begin{aligned} pst(S_4) &= \left\{\int_a^b p_{[a,t]}(nI = 1, nB = 1)[pB_1 pE_1 pRH\, \lambda_d(t)] p_{[t,b]}(nI = 0)dt\right\}\left\{p_{[0,a]}(nM = 0)\;\; p_{[a,b]}(nM \geq 1)\right\} \\ &= \left\{\int_a^b \left[\int_a^{t^-} pB_1 pE_0 \lambda_d(\tau)d\tau\right]\left[\exp\left(-\int_a^t \lambda_d(\tau)d\tau\right)\right]\left[pB_1 pE_1 pRH\, \lambda_d(t)\right]\left[\exp\left(-\int_t^b \lambda_d(\tau)d\tau\right)\right]dt\right\} \\ &\quad \left\{\left[\exp\left(-\int_0^a \lambda_m(t)dt\right)\right]\left[1 - \exp\left(-\int_a^b \lambda_m(t)dt\right)\right]\right\} \\ &= \left\{\int_a^b \left[\int_a^t \lambda_d(\tau)d\tau\right]\lambda_d(t)dt\right\}\left\{\exp\left(-\int_a^b \lambda_d(t)dt\right)\right\}\left\{pB_1^2 pE_0 pE_1 pRH\right\} \\ &\quad \left\{\exp\left(-\int_0^a \lambda_m(t)dt\right) - \exp\left(-\int_0^b \lambda_m(t)dt\right)\right\}, \end{aligned} \tag{65}$$

where

$p_{[a,\,t]}(nI = 1, nB = 1)$ = probability that exactly one intrusion (i.e., $nI = 1$) will penetrate the area marked by the berm during the time interval $[a, b]$, with this intrusion penetrating pressurized brine (i.e., $nB = 1$) but failing to penetrate an excavated area of the repository

$$= \left[\left(\int_a^t pB_1 pE_0 \lambda_d(\tau)d\tau\right)^1 \Big/ 1!\right]\left[\exp\left(-\int_a^t pB_1 pE_0 \lambda_d(\tau)d\tau\right)\right]$$

$$\left[\exp\left(-\int_a^t (pB_0 pE_0 + pE_1)\lambda_d(\tau)d\tau\right)\right]$$

$$= \left[\int_a^t pB_1 pE_0 \lambda_d(\tau)d\tau\right]\left[\exp\left(-\int_a^t \lambda_d(\tau)d\tau\right)\right] \quad (66)$$

$p_{[t,\,b]}(nI = 0)$ = probability that no intrusions (i.e., $nI = 0$) will penetrate the area marked by the berm during the time interval $[t, b]$

$$= \exp\left(-\int_t^b \lambda_d(\tau)d\tau\right) \quad (67)$$

$p_{[0,\,a]}(nM = 0)$ = probability that no mining (i.e., $nM = 0$) will occur during the time interval $[0, a]$

$$= \exp\left(-\int_0^a \lambda_m(t)dt\right) \quad (68)$$

$p_{[a,\,b]}(nM \geq 1)$ = probability that mining will occur (i.e., $nM \geq 1$) during the time interval $[a, b]$

$$= 1 - \exp\left(-\int_a^b \lambda_m(t)dt\right) \quad (69)$$

and the development of Eq. (66) is similar to that indicated for Eq. (62).

The consideration of more complex scenarios will result in more complex formulas for scenario probability. Closed-form formulas for the probabilities of quite complex scenarios can be derived but they are very complicated and involve large numbers of iterated integrals.[13] Thus, p_{st} can be defined in concept but does not have a simple form that can be easily displayed.

The example scenarios S_0, S_1, S_2, S_3, S_{21} and S_4 have infinitely many elements and nonzero probabilities. However, scenarios involving drilling intrusions that occur at specific times will have a probability of zero. For example, the scenario

$$S_5 = \{\mathbf{x}_{st}\!: \ \mathbf{x}_{st} = [t_1 = 350 \text{ yr}, l_1, e_1 = 1, b_1 = 1, p_1 = 2, \mathbf{a}_1, t_{min}], \text{ with } l_1, \mathbf{a}_1 \text{ and } t_{min} \text{ unrestricted}\} \quad (70)$$

contains infinitely many futures (i.e., infinitely many $\mathbf{x}_{st}$ meet the criteria to belong to S_5 due to the infinite number of values that t_{min} can assume) and also has a probability of zero (i.e., $p_{st}(S_5) = 0$) because t_1 is restricted to a single value. Sets that contain single elements of S_{st} are also scenarios, but such scenarios will typically have a probability of zero. In particular, the only single element scenario that has a nonzero probability contains the future that has no drilling intrusions and no mining.

The probabilities for a large number of relatively simple scenarios are given in Tables 1 and 2. Each of these scenarios can be expressed in the set notation used in this section. For example, Table 1 gives a probability of 0.102 for the scenario that involves exactly three drilling intrusions into an excavated area of the repository during the regulatory period. The corresponding scenario is

$$S = \{\mathbf{x}_{st}: \mathbf{x}_{st} \text{ involves exactly three drilling intrusions through an excavated area of the repository (i.e., } n \geq 3 \text{ in Eq. (1) and there exist integers } i, j, k \text{ such that } 1 \leq i < j < k \leq n,\ 100 \text{ yr} < t_i,\ e_i = e_j = e_k = 1, \text{ and } e_l = 0 \text{ for } l \neq i, j, k \text{ and } 1 \leq l \leq n\}. \quad (71)$$

In the definition of S, no restrictions are placed on l_m, b_m, p_m and $\mathbf{a}_m$ for $m = 1, 2, \ldots, n$ nor on t_{min} because these elements of $\mathbf{x}_{st}$ are not specified and thus can take on any values in their allowable ranges (i.e., $l_m = 1, 2, \ldots, 144$; $b_m = 0, 1$; $p_m = 1, 2, 3$; $\mathbf{a}_m$ as defined in Eqs. (11) - (13); $0 \leq t_{min} \leq 10{,}000$ yr). If one or more of these characteristics is restricted to a subset of its range, then a new scenario will be produced that is a subset of S and has, in most cases, a smaller probability than S.

The 1991 and 1992 WIPP PAs used an approach to the construction of the CCDF specified in 40 CFR 191.13 based on the exhaustive division of S_{st} into a collection of mutually exclusive scenarios $S_{st,i}$, $i = 1, 2, \ldots, nS$ (Ref. 24). A probability $p_{st}(S_{st,i})$ and a normalized release R_i were then calculated for each scenario $S_{st,i}$ and used to construct the CCDF specified in 40 CFR 191.13. Due to the complexity of the elements $\mathbf{x}_{st}$ of S_{st} (see Eq. (1)), this approach was not used in the 1996 WIPP PA. In particular, the decomposition of S_{st} into a suitable and defensible collection of scenarios $S_{st,i}$, $i = 1, 2, \ldots, n$, is quite difficult. Further, once these scenarios are defined, it is necessary to calculate their probabilities $p_{st}(S_{st,i})$, which is also not easy. Although the calculation of the probabilities $p_{st}(S_{st,i})$ is difficult, the development of an appropriate and acceptable decomposition of S_{st} into the scenarios $S_{st,i}$ is probably the greater challenge. By using the Monte Carlo approach to CCDF construction indicated in Eq. (2) and described in more detail in Sects. 10 and 11, the 1996 WIPP PA avoided the difficulties associated with decomposing S_{st} into a collection of mutually exclusive scenarios and then calculating the probabilities of these scenarios. Additional discussion of the concept of a scenario is given in Sect. 10 of Ref. 35.

15. Discussion

The characterization of stochastic uncertainty in the 1996 WIPP PA has been described. In particular, stochastic uncertainty is characterized by a probability space $(\mathcal{S}_{st}, \mathbb{S}_{st}, p_{st})$ and leads to the CCDF specified by the U.S. Environmental Protection Agency in 40 CFR 191 (Ref. 39). The only sources of stochastic uncertainty that are incorporated into the definition of $(\mathcal{S}_{st}, \mathbb{S}_{st}, p_{st})$ in the 1996 WIPP PA, and hence into the computational implementation of the analysis, are human disruptions due to drilling or mining.

The 1996 WIPP PA maintains a conceptual and computational distinction between stochastic and subjective uncertainty. The probability space $(\mathcal{S}_{su}, \mathbb{S}_{su}, p_{su})$ used to characterize subjective uncertainty is described in Ref. 35. Introduction of the probability spaces $(\mathcal{S}_{st}, \mathbb{S}_{st}, p_{st})$ and $(\mathcal{S}_{su}, \mathbb{S}_{su}, p_{su})$ provides a way to maintain a conceptual distinction between stochastic and subjective uncertainty. In the computational implementation of the analysis, random sampling is used to propagate the effects of stochastic uncertainty (i.e., to integrate over $(\mathcal{S}_{st}, \mathbb{S}_{st}, p_{st})$) and Latin hypercube sampling is used to propagate the effects of subjective uncertainty (i.e., to integrate over $(\mathcal{S}_{su}, \mathbb{S}_{su}, p_{su})$), with stochastic uncertainty giving rise to individual CCDFs and subjective uncertainty giving rise to distributions of CCDFs.

At a conceptual level, the incorporation of stochastic and subjective uncertainty into the 1996 WIPP PA can be presented quite succinctly as a double integration problem involving $(\mathcal{S}_{st}, \mathbb{S}_{st}, p_{st})$, $(\mathcal{S}_{su}\ \mathbb{S}_{su}, p_{su})$, and an appropriately defined function f (Sect. 5, Ref. 1; Ref. 47). In practice, this incorporation is an involved process that will be described in several following papers.[26 - 29, 39]

Acknowledgment

Work performed for Sandia National Laboratories (SNL), which is a multiprogram laboratory operated by Sandia Corporation, a Lockheed Martin Company, for the United States Department of Energy under contract DE-AC04-94AL85000. Review provided at SNL by M. Chavez, C. Crawford and M.S. Tierney. Editorial support provided by L. Harrison, T. Allen, and H. Radke of Tech Reps, Inc.

References

1. Helton, J.C., Anderson, D.R., Basabilvazo, G., Jow, H.-N., & Marietta, M.G., Conceptual Structure of the 1996 Performance Assessment for the Waste Isolation Pilot Plant, *Reliability Engineering and System Safety* (in this issue).

2. Galson, D.A., Swift, P.N., Anderson, D.R., Bennett, D.G., Crawford, M.B., Hicks, T.W., & Wilmot, R.D, Scenario Development for the Waste Isolation Pilot Plant Compliance Certification Application, *Reliability Engineering and System Safety* (in this issue).

3. U.S. Environmental Protection Agency, 40 CFR Part 191: Environmental Standards for the Management and Disposal of Spent Nuclear Fuel, High-Level and Transuranic Radioactive Wastes; Final Rule, *Federal Register*, 1985, **50**, 38066-38089.

4. U.S. Environmental Protection Agency, 40 CFR Part 191: Environmental Radiation Protection Standards for the Management and Disposal of Spent Nuclear Fuel, High-Level and Transuranic Radioactive Wastes; Final Rule, *Federal Register*, 1993, **58**, 66398-66416.

5. Kaplan, S. & Garrick, B.J., On the Quantitative Definition of Risk, *Risk Analysis*, 1981, **1**, 11-27.

6. Helton, J.C., Bean, J.E., Berglund, J.W., Davis, F.J., Economy, K., Garner, J.W., Johnson, J.D., MacKinnon, R.J., Miller, J., O'Brien, D.G., Ramsey, J.L., Schreiber, J.D., Shinta, A., Smith, L.N., Stoelzel, D.M., Stockman, C., & Vaughn, P., *Uncertainty and Sensitivity Analysis Results Obtained in the 1996 Performance Assessment for the Waste Isolation Pilot Plant*, SAND98-0365, Sandia National Laboratories, Albuquerque, NM, 1998.

7. Cox, D.R. & Lewis, P.A.W., *The Statistical Analysis of Series of Events*, Chapman and Hall, London, 1996.

8. Haight, F.A., *Handbook of the Poisson Distribution*, John Wiley & Sons, New York, NY, 1967.

9. Cox, D.R. & Isham, V., *Point Processes*, Chapman and Hall, London, 1980.

10. U.S. Department of Energy, *Title 40 CFR Part 191 Compliance Certification Application for the Waste Isolation Pilot Plant*, DOE/CAO-1996-2184, Volumes I-XXI, U.S. Department of Energy, Carlsbad Area Office, Carlsbad, NM, 1996.

11. Trauth, K.M. Guzowski, R.V., Pflum, C.G., & Rodriguez, R.J., Effectiveness of Passive Institutional Controls in Reducing Inadvertent Human Intrusion into the Waste Isolation Pilot Plant for Use in Performance Assessments, WIPP/CAO-96-3168, Revision 1, November 14, 1996 with Addendum of December 6, 1996, U.S. DOE WIPP, Carlsbad Area Office, Carlsbad, NM, 1996.

12. Trauth, K., Assessment of the Effectiveness of Passive Institutional Controls in Deterring Inadvertent Human Intrusion into the WIPP for the Compliance Certification Calculations - Updated Information, Memo to J. Helton, June 26, 1996, Sandia WIPP Central Files WPO # 40133, Sandia National Laboratories, Albuquerque, NM, 1996.

13. Helton, J.C., Drilling Intrusion Probabilities for Use in Performance Assessment for Radioactive Waste Disposal, *Reliability Engineering and System Safety*, 1993, **40**, 259-275.

14. WIPP PA (Performance Assessment) Department, *Preliminary Performance Assessment for the Waste Isolation Pilot Plant, December 1992*, Volumes 1-5, SAND92-0700/1-5, Sandia National Laboratories, Albuquerque, NM, 1992-1993.

15. Powers, D.W., Sigda, J.M., & Holt, R.M., Probability of Intercepting a Pressurized Brine Reservoir under the WIPP, Sandia WIPP Central Files WPO # 40199, Sandia National Laboratories, Albuquerque, NM, 1996.

16. Thompson, T.W., Coons, W.E., Krumhansl, J.L., & Hansen, F.D., Inadvertent Intrusion Borehole Permeability, Final Draft, May 20, 1996, Sandia WIPP Central Files WPO # 41131, Sandia National Laboratories, Albuquerque, NM, 1996.

17. Sanchez, L.C., Liscum-Powell, J., Rath, J.S., & Trellue, H.R., WIPP PA Analysis Report for EPAUNI: Estimating Probability Distribution of EPA Unit Loading in the WIPP Repository for Performance Assessment Calculations, Version 1.01, Sandia WIPP Central Files WPO # 43843, Sandia National Laboratories, Albuquerque, NM, 1997.

18. Sanchez, L., Drez, P.E. & Rath, J.S., Radioactive and Nonradioactive Waste Intended for Disposal at the Waste Isolation Pilot Plant, *Reliability Engineering and System Safety* (in this issue).

19. U.S. Environmental Protection Agency, 40 CFR Part 194: Criteria for the Certification and Re-Certification of the Waste Isolation Pilot Plant's Compliance With the 40 CFR Part 191 Disposal Regulations; Final Rule, *Federal Register*, 1996, **61**, 5224-5245.

20. McKay, M.D., Beckman, R.J., & Conover, W.J., A Comparison of Three Methods for Selecting Values of Input Variables in the Analysis of Output from a Computer Code, *Technometrics*, 1979, **21**, 239-245.

21. Iman, R.L. & Conover, W.J., A Distribution-Free Approach to Inducing Rank Correlation Among Input Variables, *Communications in Statistics*, 1982, **B11**, 311-334.

22. Steinberg, H.A., Generalized Quota Sampling, *Nuclear Science and Engineering*, 1963, **15**, 142-145.

23. Raj, D., *Sampling Theory*, McGraw-Hill, New York, NY, 1968.

24. Helton, J.C. & Iuzzolino, H.J., Construction of Complementary Cumulative Distribution Functions for Comparison with the EPA Release Limits for Radioactive Waste Disposal, *Reliability Engineering and System Safety*, 1993, **40**, 277-293.

25. Vaughn, P., Bean, J.E., Helton, J.C., Lord, M.E., MacKinnon, R.J., & Schreiber, J.D., Representation of Two-Phase Flow in the Vicinity of the Repository in the 1996 Performance Assessment for the Waste Isolation Pilot Plant, *Reliability Engineering and System Safety* (in this issue).

26. Berglund, J.W., Garner, J.W., Helton, J.C., Johnson, J.D., & Smith, L.N., Direct Releases to the Surface and Associated Complementary Cumulative Distribution Functions in the 1996 Performance Assessment for the Waste Isolation Pilot Plant: Cuttings, Cavings and Spallings, *Reliability Engineering and System Safety* (in this issue).

27. Stoelzel, D.M., Garner, J.W., Helton, J.C., Johnson, J.D., O'Brien, D.G., & Smith, L.N., Direct Releases to the Surface and Associated Complementary Cumulative Distribution Functions in the 1996 Performance Assessment for the Waste Isolation Pilot Plant: Direct Brine Release, *Reliability Engineering and System Safety* (in this issue).

28. Ramsey, J.L., Blaine, R., Garner, J.W., Helton, J.C., Johnson, J.D., Smith, L.N., & Wallace, M. Radionuclide and Colloid Transport in the Culebra Dolomite and Associated Complementary Cumulative Distribution Functions in the 1996 Performance Assessment for the Waste Isolation Pilot Plant, *Reliability Engineering and System Safety* (in this issue).

29. Stockman, C.T., Garner, J.W., Helton, J.C., Johnson, J.D., Shinta, A., & Smith, L.N., Radionuclide Transport in the Vicinity of the Repository and Associated Complementary Cumulative Distribution Functions in the 1996 Performance Assessment for the Waste Isolation Pilot Plant, *Reliability Engineering and System Safety* (in this issue).

30. Iman, R.L. & Helton, J.C., An Investigation of Uncertainty and Sensitivity Analysis Techniques for Computer Models, *Risk Analysis*, 1988, **8**, 71-90.

31. Iman R.L. & Helton, J.C., The Repeatability of Uncertainty and Sensitivity Analyses for Complex Probabilistic Risk Assessments, *Risk Analysis*, 1991, **11**, 591-606.

32. Helton, J.C., Johnson, J.D., McKay, M.D., Shiver, A. W., & Sprung, J.L., Robustness of an Uncertainty and Sensitivity Analysis of Early Exposure Results with the MACCS Reactor Accident Consequence Model, *Reliability Engineering and System Safety,* 1995, **48**, 129-148.

33. Stein, M. 1987, Large Sample Properties of Simulations Using Latin Hypercube Sampling, *Technometrics* **29**, 143-151.

34. Ross, S.M., *Introduction to Probability and Statistics for Engineers and Scientists*, John Wiley & Sons, New York, NY, 1987.

35. Helton, J.C., Martell, M.-A., & Tierney, M.S., Characterization of Subjective Uncertainty in the 1996 Performance Assessment for the Waste Isolation Pilot Plant, *Reliability Engineering and System Safety* (in this issue).

36. Smith, L.N., Johnson, J.D., & Helton, J.C., Analysis Package for the CCDF Construction (Task 7) of the Performance Assessment Calculations Supporting the Compliance Certification Application (CCA), AP-AAD, Analysis package, Sandia WIPP Central Files WPO # 40524, Sandia National Laboratories, Albuquerque, NM, 1996.

37. Johnson, J.D., *WIPP PA User's Manual for CCDFGF (Version 4.00),* WPO 47364, Sandia National Laboratories, Albuquerque, NM, 1997.

38. Helton, J.C., Bean, J.E., Economy, K., Garner, J.W., MacKinnon, R.J., Miller, J., Schreiber, J.D., & Vaughn, P., Uncertainty and Sensitivity Analysis for Two-Phase Flow in the Vicinity of the Repository in the 1996 Performance Assessment for the Waste Isolation Pilot Plant: Undisturbed Conditions, *Reliability Engineering and System Safety* (in this issue).

39. Helton, J.C., Anderson, D.R., Basabilvazo, G., Jow, H.-N., & Marietta, M.G., Summary Discussion of the 1996 Performance Assessment for the Waste Isolation Pilot Plant, *Reliability Engineering and System Safety* (in this issue).

40. Helton, J.C., Bean, J.E., Economy, K., Garner, J.W., MacKinnon, R.J., Miller, J., Schreiber, J.D., & Vaughn, P., Uncertainty and Sensitivity Analysis for Two-Phase Flow in the Vicinity of the Repository in the 1996 Performance Assessment for the Waste Isolation Pilot Plant: Disturbed Conditions, *Reliability Engineering and System Safety* (in this issue).

41. Wallace, M.G., Phase II FEP, NS-11, Subsidence Associated with Mining Inside or Outside the Controlled Area, Records Package, Sandia WIPP Central Files WPO # 40816, Sandia National Laboratories, Albuquerque, NM, 1996.

42. WIPP PA (Performance Assessment) Division, *Preliminary Comparison with 40 CFR Part 191, Subpart B for the Waste Isolation Pilot Plant,* December 1991, Volumes 1-4, SAND91-0893/1-4, Sandia National Laboratories, Albuquerque, NM, 1991-1992.

43. Helton, J.C., & Shiver, A.W., 1996, A Monte Carlo Procedure for the Construction of Complementary Cumulative Distribution Functions for Comparison with the EPA Release Limits for Radioactive Waste Disposal, *Risk Analysis*, **16**, 43-55.

44. Sokolnikoff, I.S. & Redheffer, R.M., *Mathematics of Physics and Modern Engineering*, 2nd edn., McGraw-Hill, New York, NY, 1966.

45. Feller, W., *An Introduction to Probability Theory and Its Applications, Volume II,* 2nd. edn., John Wiley and Sons, New York, NY, 1971.

46. Romano, J.P. & Siegel, A.F., *Counterexamples in Probability and Statistics*, Wadsworth and Brooks/Cole, Monterey, CA, 1986.

47. Helton, J.C., 1996, Probability, Conditional Probability and Complementary Cumulative Distribution Functions in Performance Assessment for Radioactive Waste Disposal, *Reliability Engineering and System Safety*, **54**, 145-163.

Figure Captions

Fig. 1. Location of berm used in passive marker system.

Fig. 2. Cumulative distribution functions for time between drilling intrusions.

Fig. 3. Distribution of radionuclide concentration (EPA units/m^3) in CH-TRU waste streams at selected times (Refs. 17, 18).

Fig. 4. Cumulative distribution functions for time to mining.

Fig. 5. Example of random sampling to generate a sample of size $nR = 5$ from $\mathbf{x} = [U, V]$ with U normal on $[-1, 1]$ (mean = 0, 0.01 quantile = −1, 0.99 quantile = 1) and V triangular on [0, 4] (mode = 1).

Fig. 6. Example of Latin hypercube sampling to generate a sample of size $nLHS = 5$ from $\mathbf{x} = [U, V]$ with U normal on $[-1, 1]$ (mean = 0, 0.01 quantile = −1, 0.99 quantile = 1) and V triangular on [1, 4] (mode = 1).

Fig. 7. Example CCDF construction from 10,000 values for $f(\mathbf{x}_{st,i})$.

Fig. 8. Example CCDF construction from 10,000 values for $f(\mathbf{x}_{st,i})$ with vertical lines added at discontinuities (i.e., between the locations of included and excluded points in Fig. 7).

Fig. 9. Example CCDF construction based on subdivision of range of $f(\mathbf{x}_{st,i})$ into bins.

Fig. 10. Example CCDF construction based on subdivision of range of $f(\mathbf{x}_{st,i})$ into bins and connection of included points.

Fig. 11. Example CCDF construction based on subdivision of range of $f(\mathbf{x}_{st,i})$ into bins, connection of included points, and termination of CCDF at largest observed consequence value (i.e., maximum value for $f(\mathbf{x}_{st})$).

Fig. 12. Comparison of plots of multiple CCDFs with individual CCDFs continued to largest observed consequence value and then extended to the abscissa (left frame) and individual CCDFs terminated at largest observed consequence value (right frame).

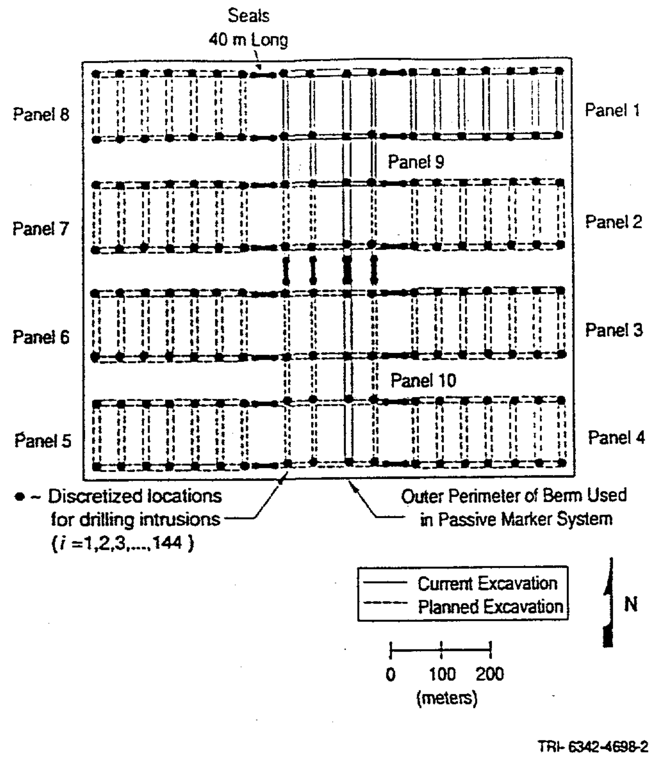

Fig. 1. Location of berm used in passive marker system.

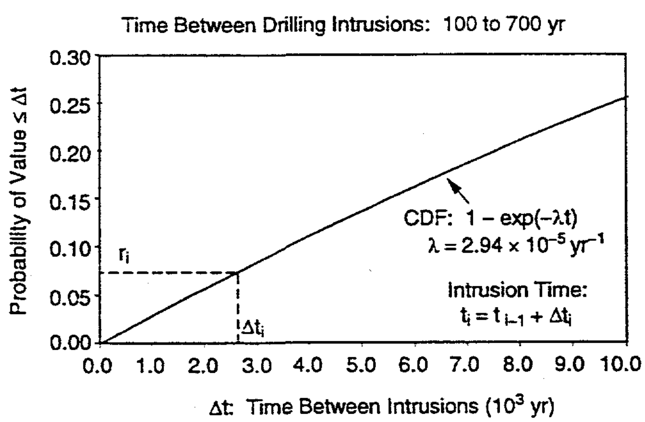

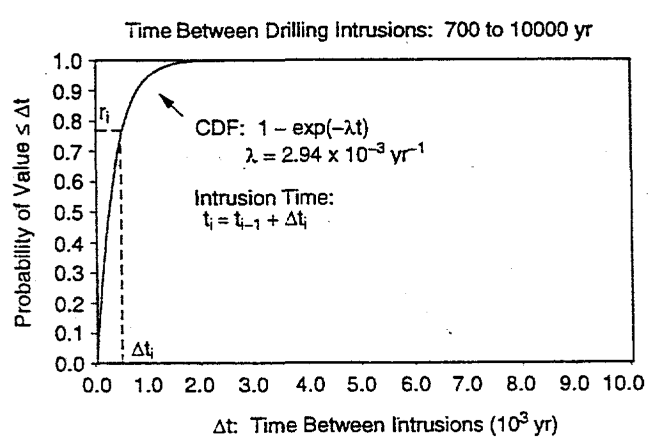

Fig. 2. Cumulative distribution functions (CDFs) for time between drilling intrusions.

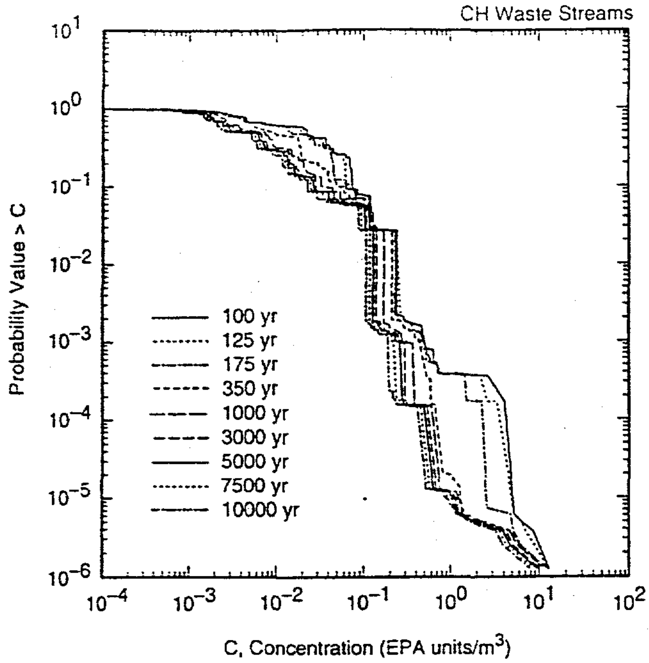

Fig. 3. Distribution of radionuclide concentration (EPA units/m^3) in CH-TRU waste streams at selected times (Refs. 17, 18).

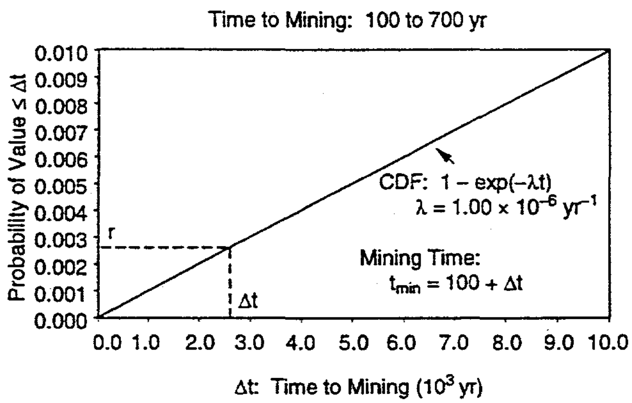

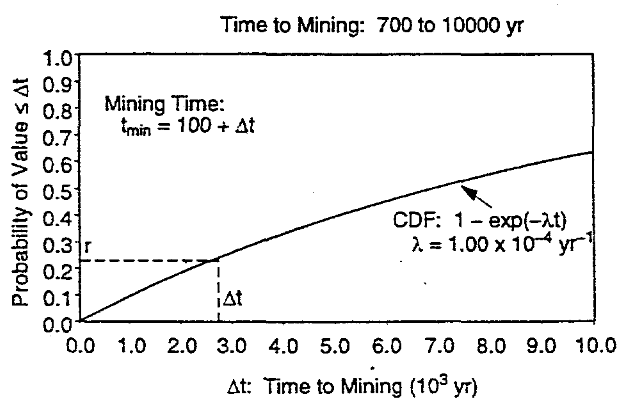

Fig. 4. Cumulative distribution functions (CDFs) for time to mining.

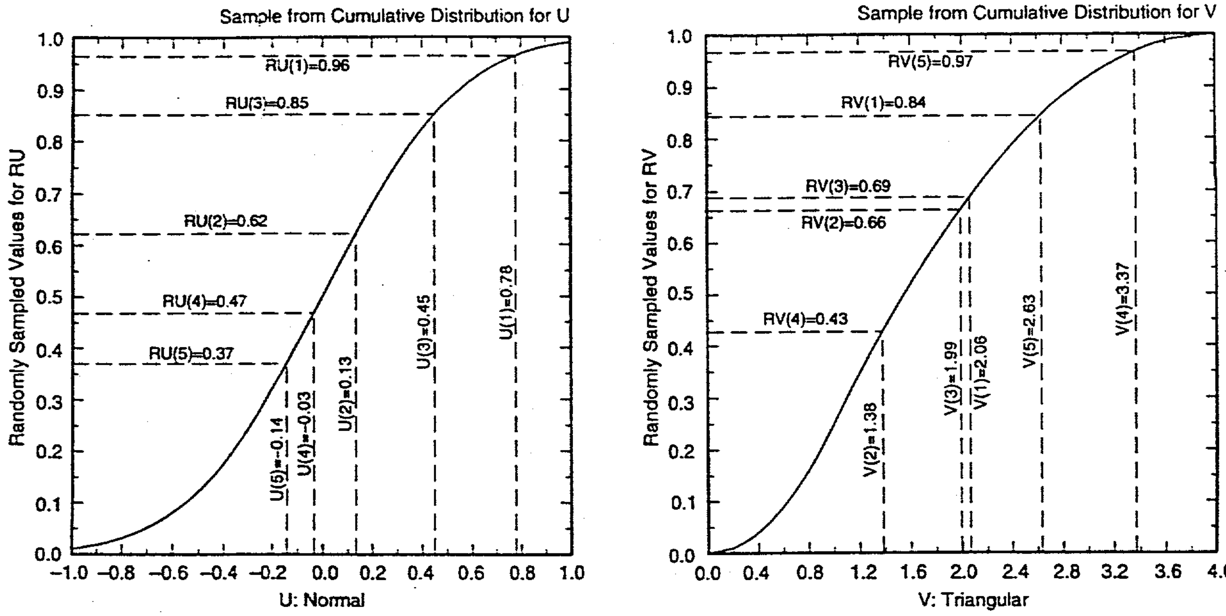

TRI-6342-5184-0A,B

Fig. 5. Example of random sampling to generate a sample of size $nR = 5$ from $\mathbf{x} = [U, V]$ with U normal on [−1, 1] (mean = 0, 0.01 quantile = −1, 0.99 quantile = 1) and V triangular on [0, 4] (mode = 1).

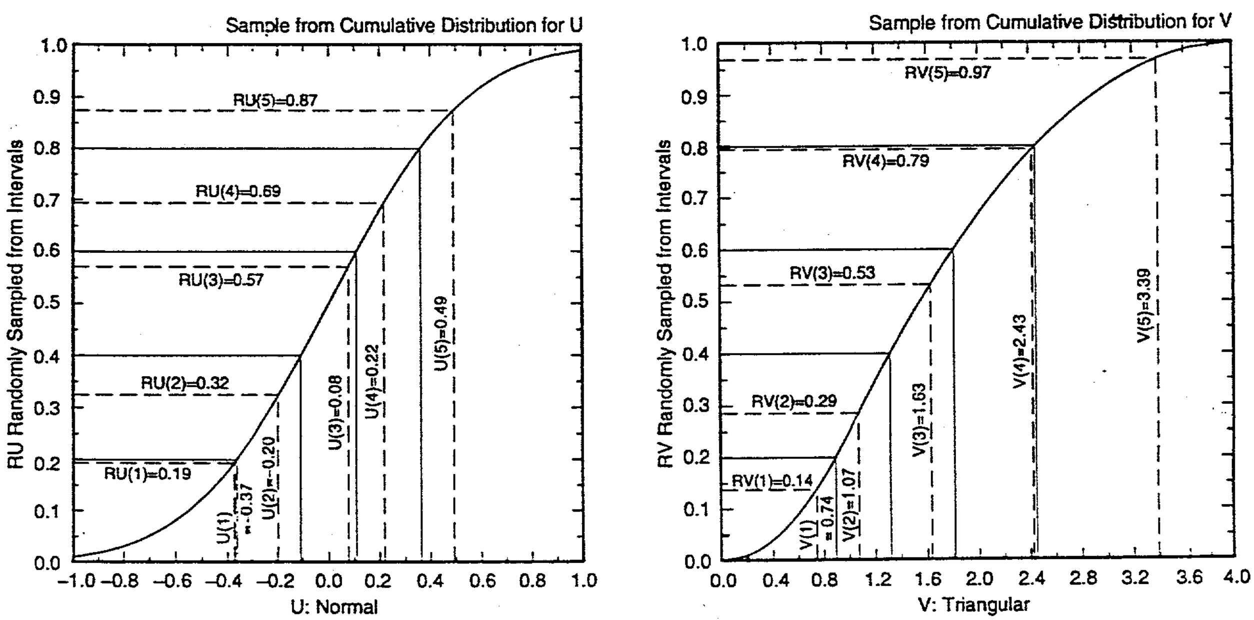

TRI-6342-5183-0A,B

Fig. 6. Example of Latin hypercube sampling to generate a sample of size $nLHS = 5$ from $\mathbf{x} = [U, V]$ with U normal on [−1, 1] (mean = 0, 0.01 quantile = −1, 0.99 quantile = 1) and V triangular on [1, 4] (mode = 1).

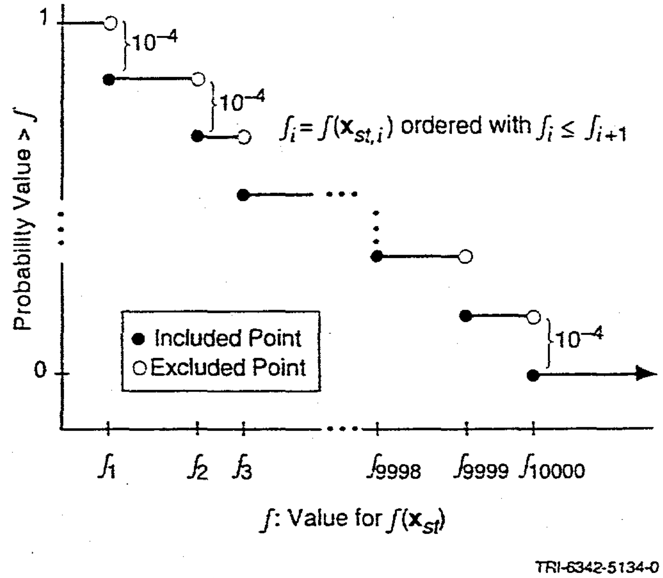

Fig. 7. Example CCDF construction from 10,000 values for $f(\mathbf{x}_{st,i})$.

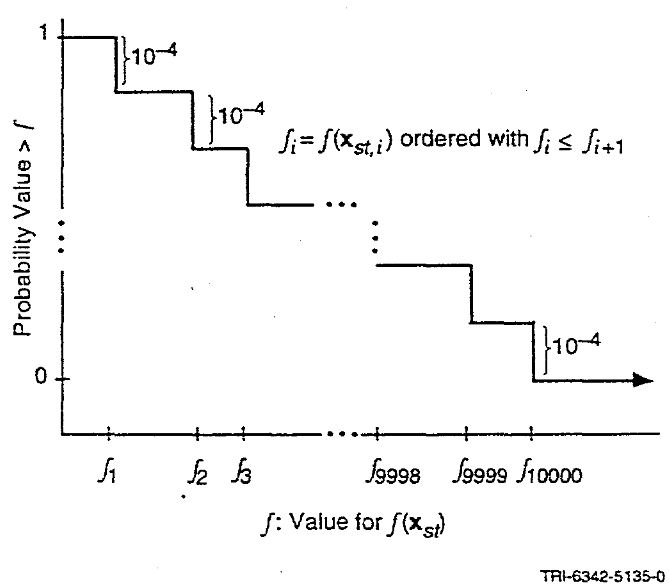

Fig. 8. Example CCDF construction from 10,000 values for $f(\mathbf{x}_{st,i})$ with vertical lines added at discontinuities (i.e., between the locations of included and excluded points in Fig. 7).

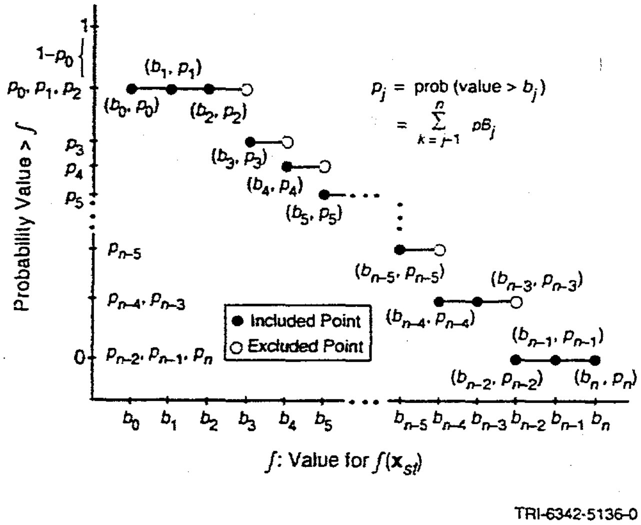

Fig. 9. Example CCDF construction based on subdivision of range of $f(\mathbf{x}_{st,i})$ into bins.

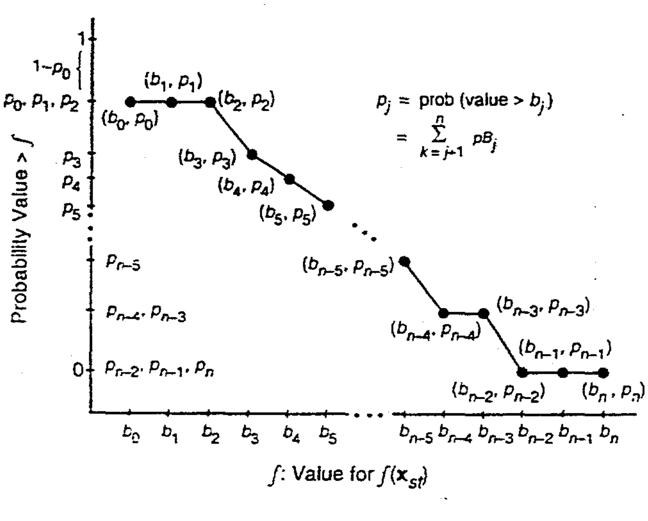

Fig. 10. Example CCDF construction based on subdivision of range of $f(\mathbf{x}_{st,i})$ into bins and connection of included points.

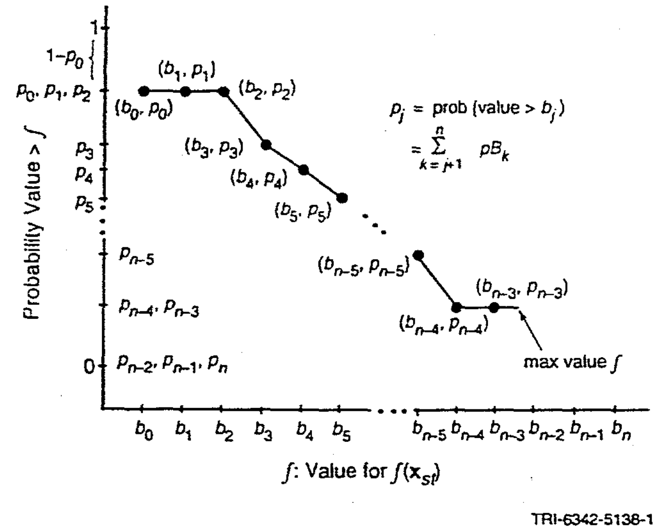

Fig. 11. Example CCDF construction based on subdivision of range of $f(\mathbf{x}_{st,i})$ into bins, connection of included points, and termination of CCDF at largest observed consequence value (i.e., maximum value for $f(\mathbf{x}_{st})$).

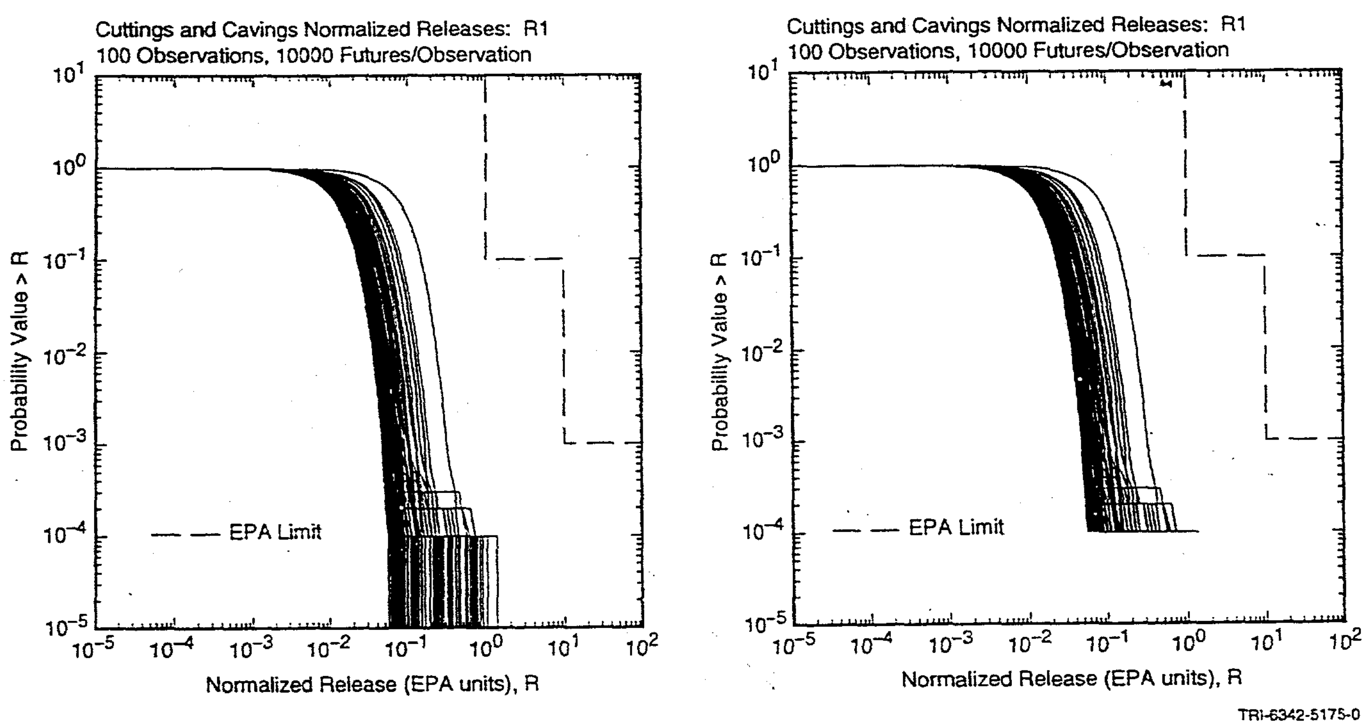

Fig. 12. Comparison of plots of multiple CCDFs with individual CCDFs continued to largest observed consequence value and then extended to the abscissa (left frame) and individual CCDFs terminated at largest observed consequence value (right frame).

Table 1. Probabilities for Futures with Different Numbers of Drilling Intrusions into the Total Area Marked by the Berm (i.e., for $\lambda_d(t)$ in Eqs. (3) - (5)) and into the Nonexcavated (i.e., $\tilde{\lambda}_d(t) = 0.791\,\lambda_d(t)$; see Sect. 4) and Excavated (i.e., $\tilde{\lambda}_d(t) = 0.209\,\lambda_d(t)$; see Sect. 4) Areas beneath the Berm

During Passive Institutional Controls: 1.00E+02 to 7.00E+02 yr

Number of Intrusions	Nonexcavated (λ_d =2.33E–05/yr)		Excavated (λ_d =6.15E–06/yr)		Total (λ_d =2.94E–05/yr)	
(n)	(=n)	($\geq n$)	(=n)	($\geq n$)	(=n)	($\geq n$)
0	9.86E–01	1.00E+00	9.96E–01	1.00E+00	9.83E–01	1.00E+00
1	1.38E–02	1.39E–02	3.68E–03	3.68E–03	1.73E–02	1.75E–02
2	9.61E–05	9.65E–05	6.78E–06	6.79E–06	1.53E–04	1.54E–04
3	4.47E–07	4.49E–07	8.34E–09	8.35E–09	9.00E–07	9.04E–07

After Passive Institutional Controls: 7.00E+02 to 1.00E+04 yr

Number of Intrusions	Nonexcavated (λ_d =2.33E–03/yr)		Excavated (λ_d =6.15E–04/yr)		Total (λ_d =2.94E–03/yr)	
(n)	(=n)	($\geq n$)	(=n)	($\geq n$)	(=n)	($\geq n$)
0	4.02E–10	1.00E+00	3.28E–03	1.00E+00	1.32E–12	1.00E+00
1	8.69E–09	1.00E+00	1.88E–02	9.97E–01	3.61E–11	1.00E+00
2	9.40E–08	1.00E+00	5.37E–02	9.78E–01	4.93E–10	1.00E+00
3	6.78E–07	1.00E+00	1.02E–01	9.24E–01	4.50E–09	1.00E+00
4	3.67E–06	1.00E+00	1.46E–01	8.22E–01	3.08E–08	1.00E+00
5	1.59E–05	1.00E+00	1.67E–01	6.76E–01	1.68E–07	1.00E+00
6	5.72E–05	1.00E+00	1.60E–01	5.08E–01	7.67E–07	1.00E+00
7	1.77E–04	1.00E+00	1.30E–01	3.49E–01	3.00E–06	1.00E+00
8	4.78E–04	1.00E+00	9.32E–02	2.18E–01	1.02E–05	1.00E+00
9	1.15E–03	9.99E–01	5.92E–02	1.25E–01	3.12E–05	1.00E+00
10	2.49E–03	9.98E–01	3.39E–02	6.60E–02	8.52E–05	1.00E+00
11	4.89E–03	9.96E–01	1.76E–02	3.21E–02	2.12E–04	1.00E+00
12	8.82E–03	9.91E–01	8.40E–03	1.45E–02	4.83E–04	1.00E+00
13	1.47E–02	9.82E–01	3.70E–03	6.09E–03	1.02E–03	9.99E–01
14	2.27E–02	9.67E–01	1.51E–03	2.39E–03	1.99E–03	9.98E–01
15	3.27E–02	9.45E–01	5.76E–04	8.82E–04	3.62E–03	9.96E–01
16	4.43E–02	9.12E–01	2.06E–04	3.06E–04	6.19E–03	9.93E–01
17	5.63E–02	8.68E–01	6.92E–05	1.00E–04	9.96E–03	9.86E–01
18	6.77E–02	8.11E–01	2.20E–05	3.12E–05	1.51E–02	9.76E–01
	...		...		...	
48	3.96E–07	7.01E–07	5.98E–28	0.00E+00	1.01E–04	2.22E–04
49	1.75E–07	3.05E–07	6.98E–29	0.00E+00	5.63E–05	1.21E–04
50	7.56E–08	1.30E–07	7.98E–30	0.00E+00	3.08E–05	6.49E–05

During Regulatory Period: 1.00E+02 to 1.00E+04 yr

Number of Intrusions	Nonexcavated[a] (λ_d =2.19E–03/yr)		Excavated[a] (λ_d =5.78E–04/yr)		Total[a] (λ_d =2.76E–03/yr)	
(n)	(=n)	($\geq n$)	(=n)	($\geq n$)	(=n)	($\geq n$)
0	3.96E–10	1.00E+00	3.27E–03	1.00E+00	1.30E–12	1.00E+00
1	8.58E–09	1.00E+00	1.87E–02	9.97E–01	3.54E–11	1.00E+00
2	9.29E–08	1.00E+00	5.35E–02	9.78E–01	4.85E–10	1.00E+00

Table 1. Probabilities for Futures with Different Numbers of Drilling Intrusions into the Total Area Marked by the Berm (i.e., for $\lambda_d(t)$ in Eqs. (3) - (5)) and into the Nonexcavated (i.e., $\tilde{\lambda}_d(t) = 0.791\,\lambda_d(t)$; see Sect. 4) and Excavated (i.e., $\tilde{\lambda}_d(t) = 0.209\,\lambda_d(t)$; see Sect. 4) Areas beneath the Berm (continued)

During Regulatory Period: 1.00E+02 to 1.00E+04 yr						
Number of Intrusions	Nonexcavated (λ_d=2.19E–03/yr)		Excavated (λ_d=5.78E–04/yr)		Total (λ_d=2.76E–03/yr)	
(n)	(=n)	(≥n)	(=n)	(≥n)	(=n)	(≥n)
3	6.70E–07	1.00E+00	1.02E–01	9.24E–01	4.43E–09	1.00E+00
4	3.63E–06	1.00E+00	1.46E–01	8.22E–01	3.03E–08	1.00E+00
5	1.57E–05	1.00E+00	1.67E–01	6.76E–01	1.66E–07	1.00E+00
6	5.67E–05	1.00E+00	1.60E–01	5.09E–01	7.57E–07	1.00E+00
7	1.75E–04	1.00E+00	1.30E–01	3.49E–01	2.96E–06	1.00E+00
8	4.74E–04	1.00E+00	9.33E–02	2.19E–01	1.01E–05	1.00E+00
9	1.14E–03	9.99E-01	5.94E–02	1.26E–01	3.08E–05	1.00E+00
10	2.47E–03	9.98E-01	3.40E–02	6.62E–02	8.43E–05	1.00E+00
11	4.86E–03	9.96E-01	1.77E–02	3.22E–02	2.10E–04	1.00E+00
12	8.77E–03	9.91E-01	8.43E–03	1.46E–02	4.78E–04	1.00E+00
13	1.46E–02	9.82E-01	3.71E–03	6.12E–03	1.01E–03	9.99E–01
14	2.26E–02	9.67E-01	1.52E–03	2.41E–03	1.97E–03	9.98E–01
15	3.26E–02	9.45E-01	5.79E–04	8.88E–04	3.59E–03	9.96E–01
16	4.41E–02	9.12E-01	2.07E–04	3.08E–04	6.15E–03	9.93E–01
17	5.61E–02	8.68E-01	6.98E–05	1.01E–04	9.90E–03	9.86E–01
18	6.75E–02	8.12E-01	2.22E–05	3.15E–05	1.51E–02	9.77E–01
	...		...		...	
48	4.03E–07	7.13E–07	6.14E–28	7.45E–17	1.02E–04	2.25E–04
49	1.78E–07	3.11E–07	7.18E–29	7.45E–17	5.71E–05	1.23E–04
50	7.70E–08	1.33E–07	8.22E–30	7.45E–17	3.13E–05	6.59E–05

[a] Rate (i.e., λ_d) is time-dependent; indicated rate is equivalent time-averaged rate (e.g., 2.76×10^{-3} yr^{-1} = (600 yr/9900 yr) (2.94×10^{-5} yr^{-1}) + (9300 yr/9900 yr)(2.94×10^{-3} yr^{-1}))

Table 2. Probabilities for Futures with Different Numbers of Drilling Intrusions that Penetrate Pressurized Brine in the Total Area Marked by the Berm (i.e., for the drilling rate $\tilde{\lambda}_d$ into pressurized brine defined by $\lambda_d(t)$ in Eqs. (3) - (5) multiplied by 0.08) and into the Nonexcavated (i.e., $\tilde{\lambda}_d(t) = (0.08)(0.791)\lambda_d(t)$) and Excavated (i.e., $\tilde{\lambda}_d(t) = (0.08)(0.209)\lambda_d(t)$) Areas beneath the Berm

Number of Intrusions	During Passive Institutional Controls: 1.00E+02 to 7.00E+02 yr					
	Nonexcavated ($\tilde{\lambda}_d$ =1.86E−06/yr)		Excavated ($\tilde{\lambda}_d$ =4.92E−07/yr)		Total ($\tilde{\lambda}_d$ =2.35E−06/yr)	
(n)	(=n)	($\geq n$)	(=n)	($\geq n$)	(=n)	($\geq n$)
0	9.99E−01	1.00E+00	1.00E+00	1.00E+00	9.99E−01	1.00E+00
1	1.12E−03	1.12E−03	2.95E−04	2.95E−04	1.41E−03	1.41E−03
2	6.23E−07	6.23E−07	4.36E−08	4.36E−08	9.95E−07	9.96E−07

Number of Intrusions	After Passive Institutional Controls: 7.00E+02 to 1.00E+04 yr					
	Nonexcavated ($\tilde{\lambda}_d$ =1.86E−04/yr)		Excavated ($\tilde{\lambda}_d$ =4.92E−05/yr)		Total ($\tilde{\lambda}_d$ =2.35E−04/yr)	
(n)	(=n)	($\geq n$)	(=n)	($\geq n$)	(=n)	($\geq n$)
0	1.77E−01	1.00E+00	6.33E−01	1.00E+00	1.12E−01	1.00E+00
1	3.07E−01	8.23E−01	2.90E−01	3.67E−01	2.45E−01	8.88E−01
2	2.65E−01	5.16E−01	6.63E−02	7.76E−02	2.68E−01	6.43E−01
3	1.53E−01	2.51E−01	1.01E−02	1.14E−02	1.96E−01	3.74E−01
4	6.62E−02	9.78E−02	1.16E−03	1.27E−03	1.07E−01	1.78E−01
5	2.29E−02	3.16E−02	1.06E−04	1.14E−04	4.69E−02	7.12E−02
6	6.61E−03	8.69E−03	8.07E−06	8.63E−06	1.71E−02	2.44E−02
7	1.64E−03	2.07E−03	5.27E−07	5.59E−07	5.35E−03	7.26E−03
8	3.54E−04	4.36E−04	3.02E−08	3.18E−08	1.46E−03	1.91E−03
9	6.80E−05	8.20E−05	1.53E−09	1.61E−09	3.56E−04	4.52E−04
10	1.18E−05	1.39E−05	7.02E−11	7.32E−11	7.78E−05	9.67E−05

Number of Intrusions	During Regulatory Period: 1.00E+02 to 1.00E+04 yr					
	Nonexcavated ($\tilde{\lambda}_d$ =1.75E−04/yr)		Excavated ($\tilde{\lambda}_d$ =4.63E−05/yr)		Total ($\tilde{\lambda}_d$ =2.21E−04/yr)	
(n)	(=n)	($\geq n$)	(=n)	($\geq n$)	(=n)	($\geq n$)
0	1.77E−01	1.00E+00	6.33E−01	1.00E+00	1.12E−01	1.00E+00
1	3.06E−01	8.23E−01	2.90E−01	3.67E−01	2.45E−01	8.88E−01
2	2.65E−01	5.17E−01	6.63E−02	7.77E−02	2.68E−01	6.43E−01
3	1.53E−01	2.51E−01	1.01E−02	1.14E−02	1.96E−01	3.75E−01
4	6.63E−02	9.80E−02	1.16E−03	1.27E−03	1.07E−01	1.79E−01
5	2.30E−02	3.17E−02	1.06E−04	1.15E−04	4.70E−02	7.14E−02
6	6.63E−03	8.71E−03	8.10E−06	8.66E−06	1.71E−02	2.44E−02
7	1.64E−03	2.08E−03	5.30E−07	5.62E−07	5.36E−03	7.28E−03
8	3.55E−04	4.38E−04	3.03E−08	3.19E−08	1.47E−03	1.92E−03
9	6.84E−05	8.24E−05	1.54E−09	1.62E−09	3.57E−04	4.54E−04
10	1.18E−05	1.40E−05	7.06E−11	7.37E−11	7.82E−05	9.72E−05

[a] Rate (i.e., $\tilde{\lambda}_d$) is time-dependent; indicated rate is equivalent time-averaged rate (e.g., 2.21×10^{-4} yr^{-1} = (600 yr/9900 yr) (2.35×10^{-6} yr^{-1}) + (9300 yr/9900 yr)(2.35×10^{-4} yr^{-1}))

Table 3. Concentrations and Conditional Probabilities for Individual Waste Streams Associated with CH- and RH-TRU Waste (Refs. 17, 18)

Waste Stream[a]	Cond Prob[b]	Concentration (EPA units/m^3) at Indicated Times (yr)								
		100	125	175	350	1000	3000	5000	7500	10000
						CH Waste				
1	7.282E-05	4.844E-03	4.654E-03	4.295E-03	3.244E-03	1.144E-03	4.630E-05	1.873E-06	3.400E-08	6.172E-10
2	1.359E-05	3.243E-03	3.159E-03	3.001E-03	2.648E-03	2.162E-03	1.702E-03	1.456E-03	1.214E-03	1.022E-03
3	2.963E-04	3.164E-03	3.133E-03	3.074E-03	2.910E-03	2.574E-03	2.244E-03	2.068E-03	1.880E-03	1.716E-03
4	9.715E-04	3.157E-03	3.126E-03	3.068E-03	2.903E-03	2.568E-03	2.239E-03	2.063E-03	1.876E-03	1.711E-03
5	5.555E-05	6.320E-03	6.258E-03	6.141E-03	5.812E-03	5.141E-03	4.482E-03	4.131E-03	3.755E-03	3.427E-03
6	4.036E-06	8.418E-01	6.934E-01	4.716E-01	1.287E-01	1.421E-02	1.281E-02	1.213E-02	1.133E-02	1.058E-02
7	1.246E-06	2.780E--1	2.290E-01	1.557E-01	4.249E-02	4.691E-03	4.228E-03	4.002E-03	3.737E-03	3.491E-03
						...				
567	1.642E-04	4.657E+00	3.826E+00	2.584E+00	6.629E-01	1.971E-02	1.307E-02	1.206E-02	1.105E-02	1.021E-02
568	1.890E-04	3.024E+00	2.484E+00	1.676E+00	4.270E-01	8.839E-03	4.744E-03	4.296E-03	3.889E-03	3.571E-03
569	3.086E-06	3.468E-01	3.465E-01	3.460E-01	3.443E-01	3.379E-01	3.190E-01	3.011E-01	2.802E-01	2.607E-01
SUM=	1.000E+00[c]									
						RH Waste				
1	1.000E+00	1.021E-02	9.421E-03	8.569E-03	7.488E-03	5.883E-03	4.659E-03	4.200E-03	3.742E-03	3.356E-03
SUM=	1.000E+00									

[a] Waste stream for indicated waste type (i.e., CH-TRU or RH-TRU)

[b] Probability of waste stream conditional on occurrence of indicated waste type (i.e., pCH_j, $j = 1, 2, \ldots, 569$, for CH-TRU waste and pRH, for RH-TRU waste)

[c] Sum of conditional probabilities

Table 4. Algorithm to Sample Time of a Drilling Intrusion with

$$\lambda(t) = \begin{cases} \mu = fPICD\,\lambda & \text{for } tA \le t \le tA + tPICD \\ \lambda & \text{for } tA + tPICD < t, \end{cases}$$

where tA = 100 yr is the time at which administrative control ends, $fPICD$ = 0.01 is the fractional reduction in the drilling rate due to passive institutional controls, and $tPICD$ = 600 yr is the time over which passive institutional controls are effective in deterring drilling intrusions.

---

1. Sample random number r from uniform distribution on [0, 1]. Then,

   $$r = 1 - \exp(-\mu \Delta t_1) \Rightarrow \Delta t_1 = [-\ln(1-r)] / \mu.$$

   Two cases:

   1.1 If $tA + \Delta t_1 \le tA + tPICD$, then $t_1 = tA + \Delta t_1$.

   1.2 If $tA + \Delta t_1 > tA + tPICD$, then sample *new* random r and determine *new* Δt_1:

   $$r = 1 - \exp(-\lambda \Delta t_1) \Rightarrow \Delta t_1 = [-\ln(1-r)] / \lambda.$$

   Then, $t_1 = tA + tPICD + \Delta t_1$.

2. Repeat process to obtain t_2. Two cases:

   2.1 If $t_1 < tA + tPICD$, then identical Step 1 except that tA is replaced by t_1, and the two cases are based on the inequalities

   $t_1 + \Delta t_2 \le t_1 + tPICD$ and $t_1 + \Delta t_2 > t_1 + tPICD$.

   2.2 If $t_1 > tA + tPICD$, then identical to Step 1.2 except that $tA + tPICD$ is replaced by t_1.

3. Repeat Step 2 to obtain $t_3, t_4, \ldots, t_{n+1}$, where t_{n+1} is the first time to exceed tM (=10,000 yr). Then, $t_1, t_2, \ldots, t_n$ are the desired times.

Table 5. Algorithm to Generate (i.e., Sample) Single Future $\mathbf{x}_{st}$ from S_{st}

1. Sample t_1 (see Table 4) with a time dependent λ_d given by

$$\lambda_d(t) = 0 \quad \text{if } 0 \le t \le tA$$
$$= fPICD\,\lambda_d \quad \text{if } tA < t \le tA + tPICD$$
$$= \lambda_d \quad \text{if } t > tA + tPICD$$

where $tA = 100$ yr (i.e., time at which administrative control ends), $tPICD = 600$ yr (i.e., time over which passive institutional controls are effective), $fPICD = 0.01$ (i.e., fractional reduction in drilling rate due to passive institutional controls) and $\lambda_d = 2.94 \times 10^{-3}$ yr^{-1} (see Sect. 2).

2. Sample l_1 with a probability of $pL_j = 6.94 \times 10^{-3}$ for each of the $j = 1, 2, \ldots, 144$ nodes in Fig. 1 (see Sect. 3).

3. Sample e_1 with a probability of $pE_0 = 0.791$ that the intrusion will be in an unexcavated area and a probability of $pE_1 = 0.209$ that the intrusion will be in an excavated area (see Sect. 4).

4. Sample b_1 with a probability of $pB_0 = 0.92$ that the intrusion will not penetrate pressurized brine and a probability of $pB_1 = 0.08$ that the intrusion will penetrate pressurized brine (see Sect. 5).

5. Sample p_1 with probabilities of $pPL_1 = 0.02$, $pPL_2 = 0.68$ and $pPL_3 = 0.30$ that plugging pattern 1, 2 or 3, respectively, will be used (see Sect. 6).

6. Increment counter nH if pressurized brine is penetrated and $p_1 = 2$ to provide a count of penetrations into pressurized brine (counter not incremented for $p_1 = 1, 3$ because of limited potential for brine depletion with these plugging patterns).

7. Reset b_1 to account for interplay between plugging pattern, brine flow in borehole, and possible depletion of pressurized brine:

   $b_1 = 0$ if $p_1 = 1$ (i.e., an intrusion that involves no long term brine flow from the brine pocket to the repository or the repository to the Culebra due to low borehole permeability)

   $= 1$ if $p_1 = 2$, drilling intrusion penetrates brine pocket and $nH \le nD$, where nD is the number of drilling intrusions required to deplete the brine pocket beneath the repository (i.e., an E1 intrusion into the brine pocket that can result in brine flow to the repository); see *BPVOL* in Table 5.2.1 for definition of nD in 1996 WIPP PA

   $= 2$ if (1) $p_1 = 2$, drilling intrusion penetrates brine pocket and $nH > nD$, (2) $p_1 = 2$ and drilling intrusion does not penetrate brine pocket, or (3) $p_1 = 3$ (i.e., an E2 intrusion)

8. Sample $\mathbf{a}_1$ (see Sect. 7).

   8.1 Penetration of nonexcavated area (i.e., $e_1 = 0$): $\mathbf{a}_1 = a_1 = 0$.

   8.2 Penetration of excavated area (i.e., $e_1 = 1$): Sample to determine if intrusion penetrates RH or CH waste with probabilities of $pRH = 0.120$ and $pCH = 0.880$ of penetrating RH and CH waste, respectively.

   8.3 Penetration of RH waste: $\mathbf{a}_1 = a_1 = 1$.

8.4 Penetration of CH waste: Use probabilities pCH_j of intersecting waste stream j, $j = 1, 2, \ldots, 569$, (see Table 3) to independently sample three intersected waste streams iCH_{11}, iCH_{12}, iCH_{13} (i.e., each of iCH_{11}, iCH_{12}, iCH_{13} is an integer between 1 and 569). Then, $\mathbf{a}_1 = [2, iCH_{11}, iCH_{12}, iCH_{13}]$.

9. Repeat steps 1 - 8 to determine properties (i.e., t_2, l_2, e_2, b_2, p_2, $\mathbf{a}_2$) of 2nd drilling intrusion.

10. Continue until $t_{n+1} > 10{,}000$ yr; the 1st n intrusions define the drilling intrusions associated with $\mathbf{x}_{st}$.

11. Sample t_{min} (see Table 4) with a time dependent λ_m given by

$$\begin{aligned} \lambda_m(t) &= 0 && \text{if } 0 \le t \le tA \\ &= fPICM\,\lambda_m && \text{if } tA < t \le tA + tPICM \\ &= \lambda_m && \text{if } tA + tPICM < t \end{aligned}$$

where $tA = 100$ yr, $tPICM = 600$ yr, $fPICM = 0.01$, $\lambda_m = 1 \times 10^{-4}$ yr^{-1} (see Sect. 8) and $tPICM$ and $fPICM$ are defined the same as $tPICD$ and $fPICD$ except for applying to mining rather than drilling.

Table 6. Mechanistic Calculations Performed for Individual Futures as Part of the 1996 WIPP PA

BRAGFLO
Individual Calculations (6 cases): E0 (i.e., undisturbed conditions); E1 at 350, 1000 yr (i.e., drilling intrusion through repository that penetrates pressurized brine in the Castile Fm); E2 at 350, 1000 yr (i.e., drilling intrusion through repository that does not penetrate pressurized brine in the Castile Fm); E2E1 with E2 intrusion at 800 yr and E1 intrusion at 2000 yr. *Total calculations*: 6 nR^a $nLHS^b$ = 6 • 3 • 100 = 1800. *Note:* All intrusions are represented by region 1 in Fig. 1 of Ref. 25. *Additional information*: Refs. 25, 29, 38.
CUTTINGS_S
Individual Calculations (52 cases): Intrusion into lower waste panel in previously unintruded (i.e., E0 conditions) repository at 100, 350, 1000, 3000, 5000, 10,000 yr; Intrusion into upper waste panel in previously unintruded repository at 100, 350, 1000, 3000, 5000, 10,000 yr; Initial E1 intrusion at 350 yr followed by a second intrusion into the same waste panel at 550, 750, 2000, 4000 or 10,000 yr; Initial E1 intrusion at 350 yr followed by a second intrusion into a different waste panel at 550, 750, 2000, 4000 or 10,000 yr; Initial E1 intrusion at 1000 yr followed by a second intrusion into the same waste panel at 1200, 1400, 3000, 5000 or 10,000 yr; Initial E1 intrusion at 1000 yr followed by a second intrusion into a different waste panel at 1200, 1400, 3000, 5000 or 10,000 yr; same 23 cases for initial E2 intrusions as for initial E1 intrusions. *Total calculations*: 52 *nR nLHS* = 52 • 3 • 100 = 15,600. *Note*: The calculations for two intrusions into the same waste panel assume that the intrusions are into the lower waste panel (i.e., region 23 in Fig. 1 of Ref. 25; the calculations for two intrusions into different waste panels assume that the first intrusion is into the lower waste panel (i.e., region 23 in Fig. 1 of Ref. 25 and that the second intrusion is into an upper waste panel (i.e., region 24 in Fig. 1 of Ref. 25. *Additional information*: Ref. 26.
BRAGFLO_DBR
Same computational cases as for CUTTINGS_S. *Additional information*: Ref. 27.
NUTS
Individual Calculations (15 cases): E0; E1 at 100, 350, 1000, 3000, 5000, 7000, 9000 yr; E2 at 100, 350, 1000, 3000, 5000, 7000, 9000 yr. *Screening calculations*: 5 *nR nLHS* = 1500. *Total* NUTS *calculations*: 594. *Note*: Screening calculations were initially performed for each LHS element (i.e., E0, E1 at 350 and 1000 yr, E2 at 350 and 1000 yr, which produces the multiplier of 5 in the calculation of the number of screening calculations) to determine if the potential for a radionuclide release existed, with a full NUTS calculation only being performed when such a potential existed. For the three replicates 9, 62, 67, 18 and 18 sample elements were screened in for full NUTS calculations for the cases E0, E1 at 350 yr, E1 at 1000 yr, E2 at 350 yr and E2 at 1000 yr, respectively. In turn, this lead to 9 + 62(2) + 67(5) + 18(2) + 18(5) = 594 full NUTS calculations, where the multipliers of 2 and 5 appear due to the use of intrusion results at 350 yr for NUTS calculations for intrusions at 100 and 350 yr (i.e., a multiplier of 2) and the use of intrusion results at 1000 yr for NUTS calculations for intrusions at 1000, 3000, 5000, 7000, and 9000 yr (i.e., a multiplier of 5). *Additional information*: Ref. 29.
PANEL
Individual Calculations (7 cases): E2E1 at 100, 350, 1000, 2000, 4000, 6000, 9000 yr. *Total calculations*: 7 *nR nLHS* = 7 • 3 • 100 = 2100. *Note*: Additional PANEL calculations were also performed at 100, 125, 175, 350, 1000, 3000, 5000, 7500 and 10,000 yr for Salado-dominated brines and also for Castile-dominated brines to determine dissolved radionuclide concentrations for use in the determinations of direct brine releases. *Additional information*: Ref. 29.
SECOFL2D
Individual Calculations (2 cases): Partially mined conditions in vicinity of repository (i.e., conditions before t_{min}); Fully mined conditions in vicinity of repository (i.e., conditions after t_{min}). *Total calculations*: 2 *nR nLHS* = 2 • 3 • 100 = 600. *Additional information*: Ref. 28.

Table 6. Mechanistic Calculations Performed for Individual Futures as Part of the 1996 WIPP PA (Continued)

SECOTP2D
Individual Calculations (2 cases): Partially mined conditions in vicinity of repository; Fully mined conditions in vicinity of repository. *Total calculations*: 2 *nR nLHS* = 2 • 3 • 100 = 600. *Note*: Each calculation is for four radionuclides: Am-241, Pu-239, Th-230, U-234. Further, calculations are done for unit releases at time 0 yr, which can then be used to construct transport results for the Culebra for arbitrary time-dependent release rates into the Culebra (Sect. 9 Ref. 28). *Additional information*: Ref. 28.

[a] *nR* = 3 ~ number of replicated LHSs used in analysis (Sect. 8, Ref. 35).
[b] *nLHS* = 100 ~ size of each LHS (Sect. 8, Ref. 35).